1970

Surface energy determinations in plexiglas

Li-King Chen

SURFACE ENERGY DETERMINATIONS IN PLEXIGLAS

BY

LI-KING CHEN, 1938

A

THESIS

submitted to the faculty of the

UNIVERSITY OF MISSOURI — ROLLA

in partial fulfillment of the requirement for the

Degree of

MASTER OF SCIENCE IN MINING ENGINEERING

Rolla, Missouri

1970

Approved by

David A. Summers
(Advisor)

ABSTRACT

Under irreversible conditions an effective surface energy of plexiglas for notched bars deformed in three-point bending was measured. The various equations proposed for evaluating surface energy are described and values of surface energy obtained using these equations are reported for a variety of sample dimensions. A comparison has been made between the results obtained. The effect of different notch shapes, sharp V, square U and round, on calculated values and fracture characteristics are noted. The Griffith theory is shown to be valid for large crack dimensions.

ACKNOWLEDGEMENTS

The author wishes to thank Dr. David A. Summers, Assistant Professor of Mining Engineering and Research Associate of the Rock Mechanics & Explosives Research Center, and Dr. George B. Clark, Director of the Rock Mechanics & Explosives Research Center for their advice, support, and encouragement during the course of this investigation.

This project was carried out under a Project Themis Grant from the Department of Defense, contract no DACA 45-69-C-0087.

TABLE OF CONTENTS

LIST OF FIGURES

Figures Page

Figure Page

Figure Page

LIST OF TABLES

I. INTRODUCTION

When a solid is fractured under an effective stress the work required to produce a unit increase in new surface may be defined as the surface energy. It is a measure of the density and strength of broken atomic bonds on the fracture surface. Surface energy plays a very important part in the science of solids. Many physical properties of a solid are related to its surface energy. Once the surface energy has been determined it may be possible to establish failure loads for a given specimen. Also the value of surface energy may be useful in comminution studies and studies of the energy partitioning in rock drilling.

Based on Griffith's theory several different methods of evaluating surface energy have been proposed, this thesis compares these and discusses the validity of each, as well as the validity of the basic Griffith approach. Evaluation was made through a series of experiments varying specimen dimensions, crack length, and crack shape to obtain the most applicable mathematical expression.

II. REVIEW OF LITERATURE

The literature survey is made up of two parts: (I) General Survey, (II) Statement of the equations available for surface energy evaluation. The former provides a background to the theory of surface energy determination, which is then used in the second part as a basis for theoretical evaluation through the use of differing techniques.

(I) General Survey

1. Elastic Anisotropy

There is no anisotropy of physico-mechanical properties, when a crystal has no cleavage plane, thus it is possible to speak of a single surface energy which is equal for all faces.

The surface energy for a single cleavage crystal can be considered on that plane. The anisotropy can be fully defined by the direction of forces tending to break up the crystal with respect to the cleavage plane. When the crystal has two or more cleavage planes with different degrees of perfection, the anisotropy of its properties is defined by the orientation of the forces acting on the crystal associated with the cleavage planes. To define the anisotropy of different physico-mechanical properties, it is necessary to know the surface energies of the various cleavage planes. For this reason investigators use rock types, charact-

erized by homogeneity of strength and deformation chacteristics and selected with care in order to reduce the influence of non-homogeneity and anisotropy on the mechanism of rock fracture.

2. The Griffith Theory

According to Griffith Theory (1), the theoretical strength is that microscopic fracture stress which is actually reached in a small volume of the specimen around the tip of a flaw, while the mean specimen stress may remain very low. In calculating the stress concentration at the tip of the crack length Griffith made use of Inglis' calculation(2) of the stress distribution around an elliptical hole in a stressed plate, considering the crack to be such a flat elliptical hole. If a plate containing a flat elliptical hole of major axis 2C is subjected to a tensile stress σ perpendicular to the major axis, the highest tensile stress will occur at the ends of the major axis and can be given by

$$\sigma_m = 2\sigma(C/\rho)^{1/2}$$

where σ_m becomes infinite as ρ decreases to zero and ρ is the radius of curvature at the ends of the major axis. Therefore no definitive value for σ_m can be obtained.

Griffith assumed that a crack will lengthen and cause a fracture if for an increment in its length, 2C, the work of the external force is enough to include the increase in elastic energy around the crack tip

and the "surface energy" of the crack surface area created. A surface crack of depth C results in a stress concentration approximately equal to that of an internal crack of length 2C. The excess elastic energy of the plate with a crack, relative to the energy contained by the same plate without the crack, is

$$W_e = \pi C^2 \sigma^2 / E$$

per unit of thickness, if it is small compared with the crack length, 2C, and assuming a state of plane stress. In the case of a large thickness compare with 2C, generating plane strain conditions, the excess elastic energy W_e, is calculated thus:

$$W_e = (1-\nu^2)\pi C^2 \sigma^2 / E$$

where, ν is Poissons' ratio.

The work done by the external force (W_e) when a crack length 2C is created in the specimen can be equated, for an energy balance, to the surface energy,

$$W_s = 4\gamma C$$

per unit plate thickness. The crack is in unstable equilibrium with the external force if for an incremental increase in length the surface energy and the excess elastic energy are equal to the work done by the external forces. If

$$\frac{d(W_e - W_s)}{dC} = \frac{2\pi C\sigma^2}{E} - 4\gamma = 0$$

or $$\sigma = (2\gamma E/\pi C)^{1/2}$$

for a thin plate. The corresponding condition for a thick plate is

$$\sigma = (2\gamma E/\pi C(1-\nu^2))^{1/2}$$

the crack will start to grow and fracture will occur as soon as the stress exceeds the value given by the above relationship.

3. Crack Extension

Griffith (1) compared the work required to extend a crack with the release of stored elastic energy which accompanies crack extension:

$$\frac{de}{dA} = \frac{d}{dC}\left(\frac{\pi \sigma^2 C^2}{E}\right)$$

$$\frac{dW}{dA} = \frac{d}{dC}(4C\gamma)$$

When $\frac{de}{dA} > \frac{dW}{dA}$, the crack develops rapidly, driven by release of the strain energy de and, including the work done in plastic deformation, 'effective' surface energy can be defined as

$$\gamma = \frac{dU}{dA}$$

The rate of crack growth changes as the crack increases in size, dependent on the value of $\frac{d^2U}{dA^2}$. If it is positive, the crack growth rate will increase, because the energy being released is more than sufficient to creat the new surface area, if it is negative,

there exists a point that $\frac{de}{dA}$ becomes less than $\frac{dW}{dA}$ and more external work must be done to keep the crack moving.

4. Plastic Flow

Brace and Walsh (3) indicated that measurements of surface energy of minerals have been made, but only with some difficulty. One reason is that surface energy per unit of surface area is a very small quantity. It is difficult to design an experiment in which new surface is produced and where values for the surface energy may be obtained separate from the usually much larger quantities of energy which are involved in producing plastic flow. Thus, Gilman (4) carried out experiments at temperatures down to -196°C to avoid plastic flow of his materials, but even so it was difficult to accurately measure the new surface area created.

Chang (5) indicated that the plastic strain associated with cleavage fracture arises both before and at the moment of fracture, the strain energy has, correspondingly, two components. The work done in creating new surface will include the energy of the local plastic flow due to slip at the tip of the propagation crack (W_p) and the energy of formation of a cleavage crack step (W_s). The surface energy (γ) and the kinetic energy (W_{ke}) also contribute to the fracture process. An effective surface energy (γ_{eff}) for the whole of the energy involved in promoting fracture will be therefore

$$\gamma_{eff} = \gamma + \gamma_p + W_{ke} = \gamma + W_p + W_s + W_{ke}$$

Of these component energies, γ_p is found to be greater than twice the magnitude of γ; W_p is about equal to γ; W_s is ten to hundred times as large as γ (6): Gilman (4) evaluated total effective surface energy and reported that it varies with temperature due to a change in the resistance to plastic deformation (W_p).

5. Crack Tip Effects

Irwin (6), considering Sneddon's result of 1946 (7) for the stress distribution around a penny-shaped crack, examined the stress field in the area of the crack tip. He noted that the crack tip stresses which were due to the conditions of the generalized plane stress of plane strain can be expressed by a set of two-parameter equations. These parameters, he called the stress-intensity factors (K_{ic}). The critical values of these factors, which are functions of the applied loads and the dimensions of the crack, may be determined by experiment for different materials and define the unstable crack propagation condition. The strain energy release rate, or crack extension force, which describes the loss of energy from the strain energy of the crack system with the advance of the crack, can be associated with the concept of a stress-intensity factor. While the determination of this energy release rate requires only the stress and displacement fields in a

small zone around the crack tip, it can be related to the strain energy of the Griffith theory which is established by considering the system as a whole. The linear elasticity solution for a sharp crack gives rise to infinite stresses at the crack point where the radius of the curvature is zero, and the deformed crack shape acquires at the tip of a finite curvature, while the stress levels are always lower than some ultimate stress level. Hence , it is likely that any large deformation theory could be used to predict finite stresses at the crack tip, where the radius of curvature at the end of the crack in the undeformed state is assumed to be small but not zero.

In appropriate circumstance, the K_{ic} value of a material can be used to estimate the load that a structural member containing a crack of known dimensions will sustain before fracture. Sullivan (8) has indicated that in sharply notched sheet fracture specimens under load, crack extension is often signaled by an abrupt readily discernible burst of growth from the notch tip and this been called the 'pop in' of fracture growth. Fracture toughness, calculated under known conditions of plane strain, is given as

$$K_{ic}^{2} = \frac{E\, G_{ic}}{1 - \gamma^{2}}$$

It has established for a number of materials that K_{ic} is independent of size and form of specimen when properly measured. This means, among other things, when any plastic zone generated is

considerably less than the specimen thickness (9).

(II) Comparison of the Surface Energy Values generated by Different Equations

1. Equation 1.

This equation is based on the initial assumption (1) that the total external energy input to the specimen prior to failure is absorbed in the creation of new crack surface as the crack grows and that the load deflection curve for the external force is as shown in Fig. 1. It is also assumed that plastic energy and kinetic energy absorbed per unit crack area remain constant

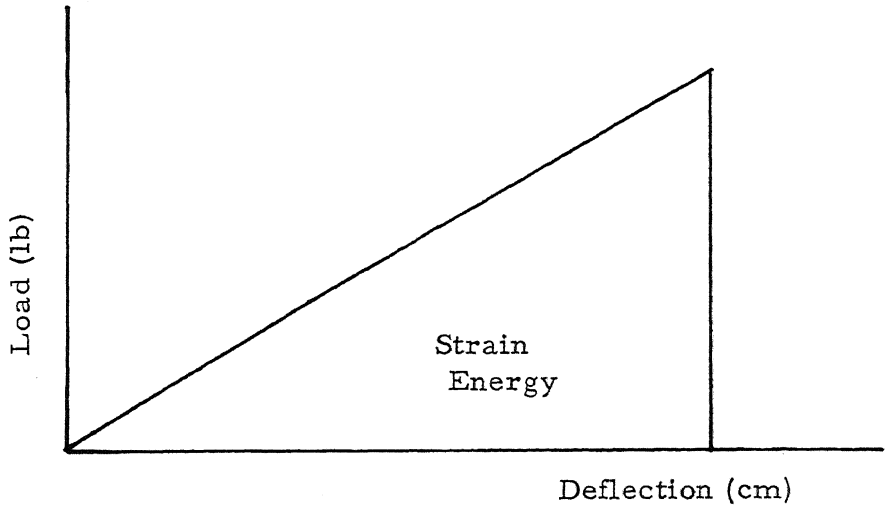

Figure 1. Load/Deflection curve for determining strain-energy release rate

$$\gamma = \frac{\text{Strain Energy}}{\text{Area Created}}$$

$$= \frac{P\delta / 2}{2b(C_f - C)}$$

$$= \frac{P\delta}{4b(C_f - C)}$$

2. Equation 2.

In a load-deflection curve where the crack does not grow completely through the specimen the curve obtained is often similar to that of Fig. 2. The plastic energy stored is generally a very small quantity and will accordingly be neglected. The total energy absorbed can be given by the area ABCD, and the plastic energy by area DEC, thus the strain energy absorbed in the creation of new surface = Area ABE - Area ACE = $P_m \delta/2 - P_r \delta/2$

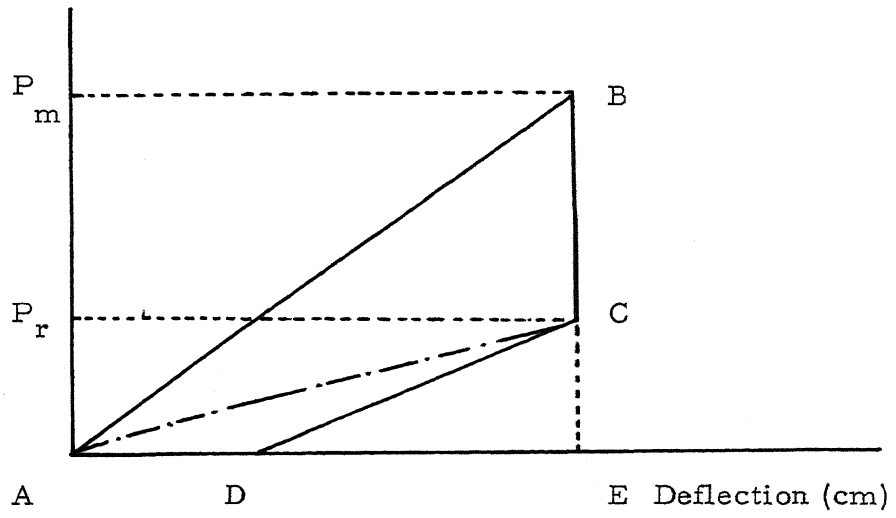

Figure 2. Load/Deflection curve for determination of strain-energy release rate without plastic energy involved

$$\text{Surface energy} = \frac{\text{Strain Energy}}{\text{Area Created}}$$

$$= \frac{P_m \delta /2 - P_r \delta /2}{2\, b\, (C_f - C)}$$

$$= \frac{\delta\, (P_m - P_r)}{4\, b\, (C_f - C)}$$

3. Equation 3.

This equation assumes the stress situation for crack initiation is that given by Griffith (1) and that the basic simple beam equation holds for the uncracked height of the specimen. From Griffith theory, the critical stress is equal to $(2E\gamma/\pi C)^{1/2}$, giving

$$\gamma = \frac{\pi\, \sigma^2\, C}{2\quad E}$$

and

$$\sigma = \frac{M\, Y}{I}$$

$$M = \frac{P\, L}{4}$$

From Fig. 3, we get,

$$Y = \frac{d - C}{2}$$

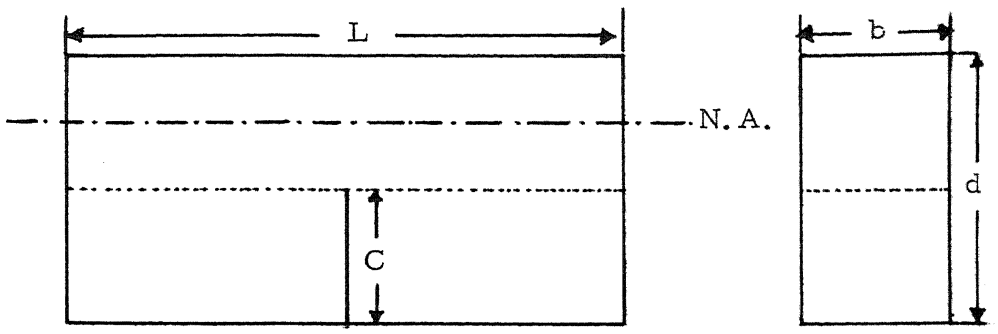

Figure 3. Specimen configuration

$$I = \frac{b\,h^3}{12} = \frac{b\,(d-C)^3}{12}$$

Therefore, by substitution in the surface equation

$$\gamma = \frac{9\pi P^2 L^2 C}{8 E b^2 (d-C)^4}$$

If the assumptions are valid this equation should hold no matter what the length of the crack. It has been shown however that where the crack is longer than 0.1 times the specimen height that the basic assumption relating to the position of the neutral axis does not hold (e.g., using finite element techniques Summers (10) has found a shift in the position of the neutral axis from the "beam center" assumed). To correct for the increased inaccuracy of the method several investigators have introduced functions of the ratio of the original notch depth to the height of the specimen, (C/d), the crack penetration ratio.

4. Equation 4.

This equation is given by Liebowitz (11) who evaluated surface

energy as

$$\gamma = \frac{9\ P^2\ L^2\ f(C/d)}{8\ E\ b^2\ (d-C)^3}$$

In its simplest form where (C/d) is small, f(C/d) is equal to $C(d-C)^3/d^4$ which reduces the equation to equation 3. At large values the function changes and several investigators have given different values. Table I, and Table II show two sets of values for the functions as given by Paris and Sih (12), and by Bueckner (13), with change in crack penetration ratio.

Table I. Value of the function given by Paris (12) for determination of the stress-intensity factor

C/d	f(C/d)
0.05	0.36
0.10	0.49
0.20	0.60
0.30	0.66
0.40	0.69
0.50	0.72
0.60	0.73

Table II. Value of the function given by Bueckner (13) for determination of the stress-intensity factor

C/d	f(C/d)
0.05	0.25
0.10	0.48
0.20	0.60
0.30	0.66
0.40	0.70
0.50	0.72
0.60	0.72

To interpolate between the values graphs have been plotted in Fig. 4 and Fig. 5.

5. Equation 5.

Srawley and Brown (14) give the surface energy value in the form

$$\gamma = \frac{P^2 L^2}{2E b^2 d^3} \left(31.7(C/d) - 64.8(C/d)^2 + 211(C/d)^3 \right).$$

based on the work of Gross (15). This equation has since been up-dated by Srawley (14) to give,

6. Equation 6.

The stress intensity factor is given in the form of the relationship

$$K_{ic} bd^2 / 6\,MC^{1/2} = A_o + A_1 (C/d) + A_2 (C/d)^2 + A_3 (C/d)^3 + A_4 (C/d)^4$$

From this equation surface energy may be derived as

$$\gamma = \frac{9\,P^2 L^2\,C}{8\,E\,b^2\,d^4} \left(A_o + A_1(C/d) + A_2(C/d)^2 + A_3(C/d)^3 + A_4(C/d)^4 \right)^2$$

where the values of A_i (i = 0, 1, 2, 3, 4) have been assumed from the values given by Srawley to be

$$A_o = 1.90 + 0.0075(L/d)$$

$$A_1 = -3.39 + 0.08(L/d)$$

$$A_2 = 15.40 - 0.2175(L/d)$$

$$A_3 = -26.24 + 0.2815(L/d)$$

$$A_4 = 26.38 - 0.145(L/d)$$

7. Equation 7.

Bueckner (13) treated the notched beam as a boundary value problem and found that the stress intensity factor K_{ic} could be given by:

$$K_{ic} = \frac{6M}{d^2} \left(\frac{2d}{\pi} \cdot h(C/d) \right)^{1/2}$$

thus,

$$\gamma = \frac{K_{ic}^2}{2\,E} = \frac{9\,P^2\,L^2}{4\,E\,d^3}\, h(C/d)$$

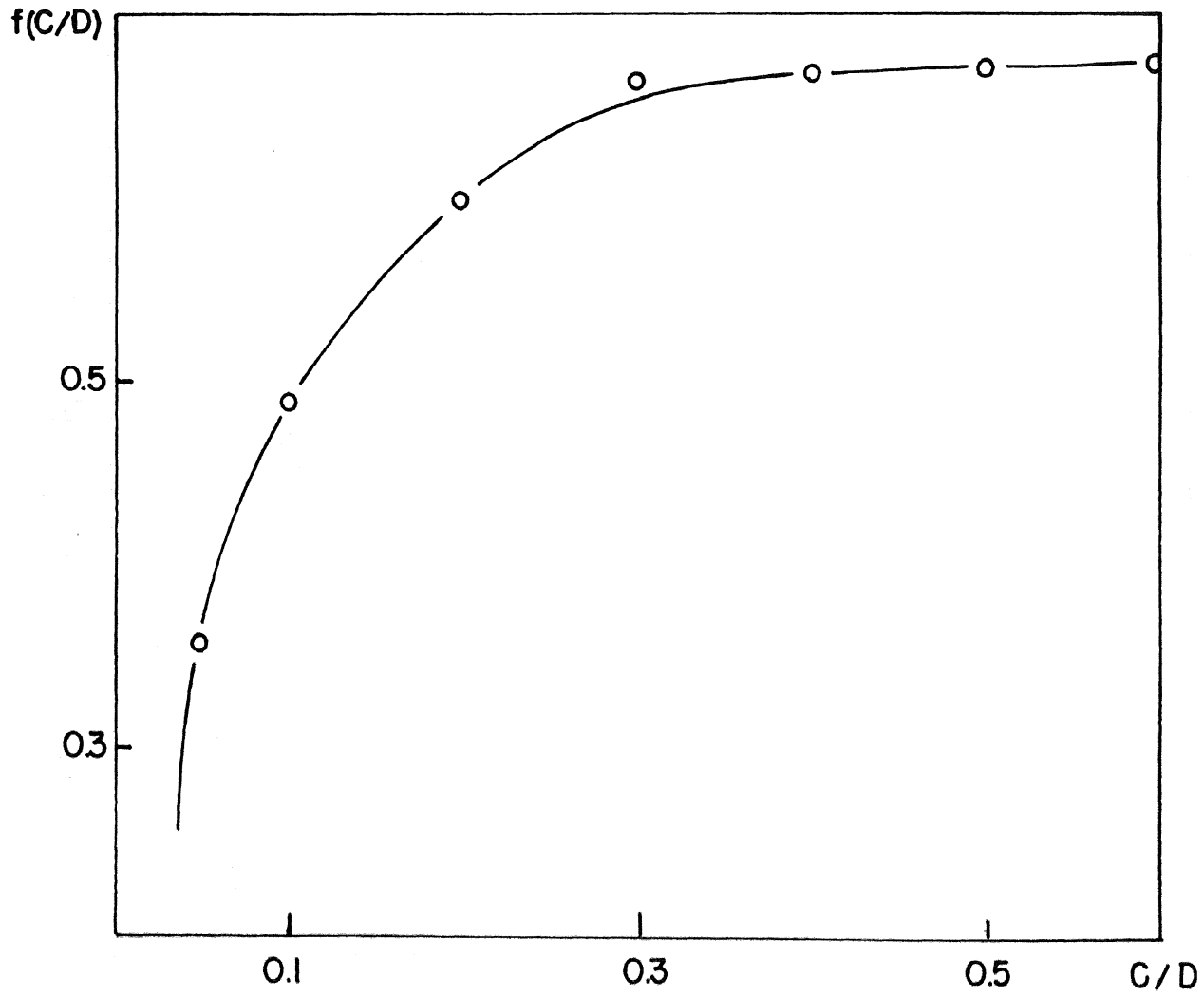

Figure 4.

Variation of crack length/height ratio stress-intensity functions, with changing ratio, given by Paris (16)

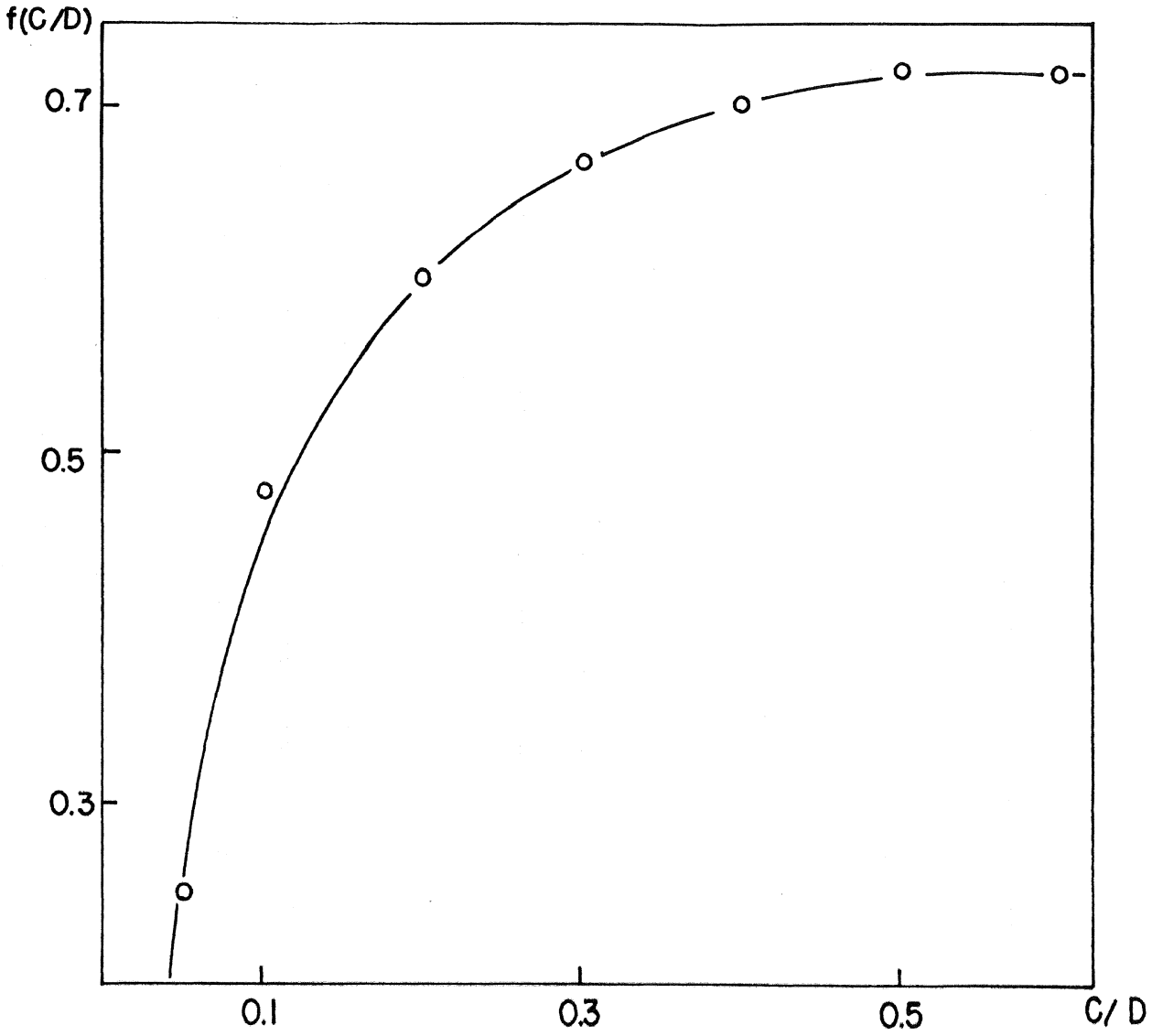

Figure 5.

Variation of crack length/height ratio stress-intensity functions, given by Bueckner (17)

Values of the functions given by Bueckner, for the determination of the stress intensity factor are shown in the following Table.

Table III. Functions given by Bueckner (13) for the determination of the stress intensity factor

C/d	$h(C/d) \cdot \frac{9}{4\pi}$
0.10	0.072
0.20	0.250
0.50	1.500

To establish values outside those given above a graph has been plotted in Fig. 6.

8. Equation 8.

Davidge and Tappin (16) considered the variation in individual results obtained and used this derivation to evaluate the surface energy based on measuring the total energy released when a notched specimen has been broken.

The load/deflection relationship is given by $P = K\delta$, and the stored energy can be given as:

$$U = \frac{P\delta}{2} = \frac{K\delta^2}{2},$$

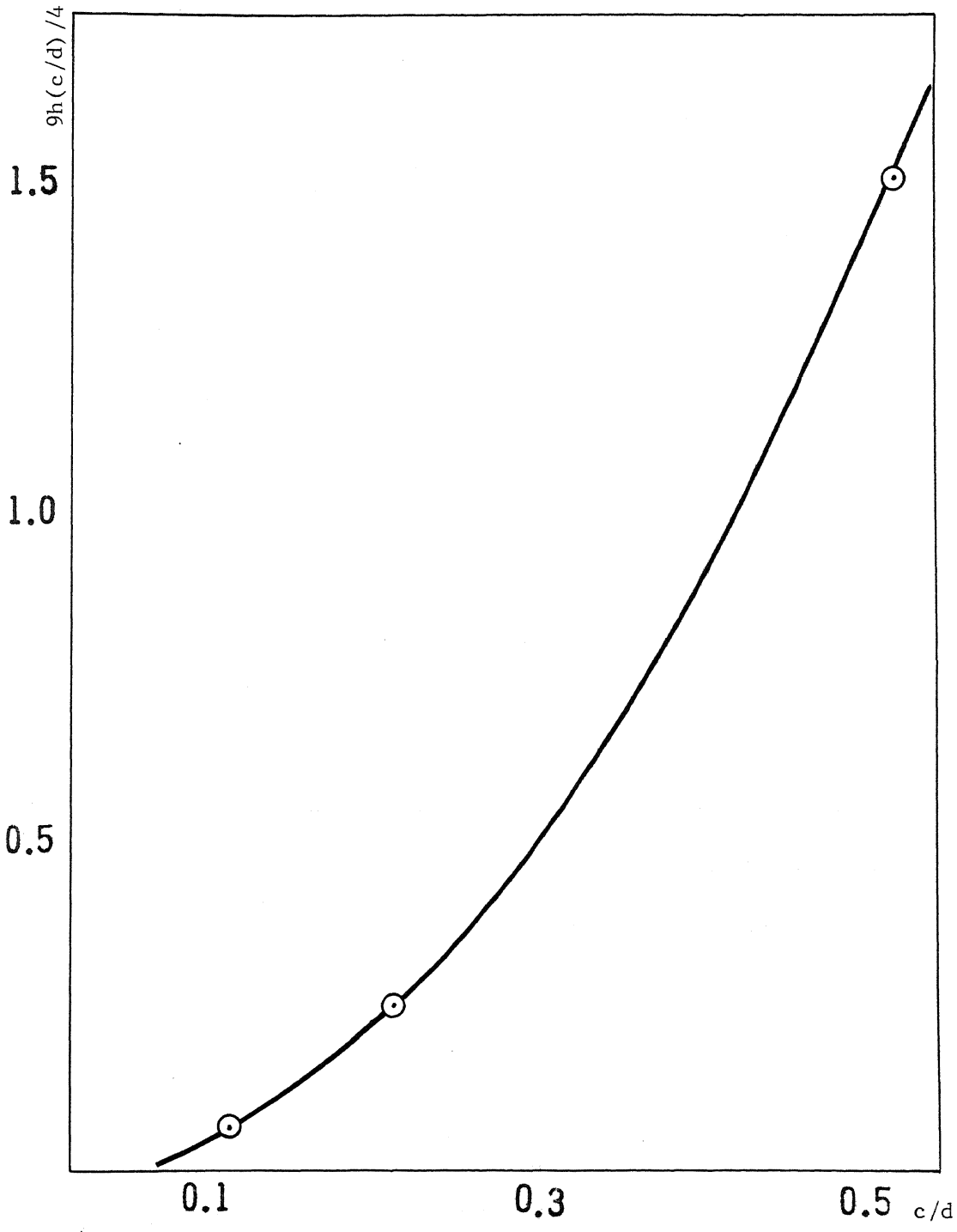

Figure 6. Variation of crack length/height ratio stress-intensity function, given by Bueckner

but, surface energy = - (dU/dA), and

$$(dU/dK) = \delta^2/2 \quad , \text{ thus,}$$

$$\gamma = -\delta^2 (dK/dA)/2$$

The value of (dK/dA) is obtained from the slope of the curve at the appropriate value of A (Fig. 7) and, with the value obtained from the experiment for δ, the surface energy value may be obtained.

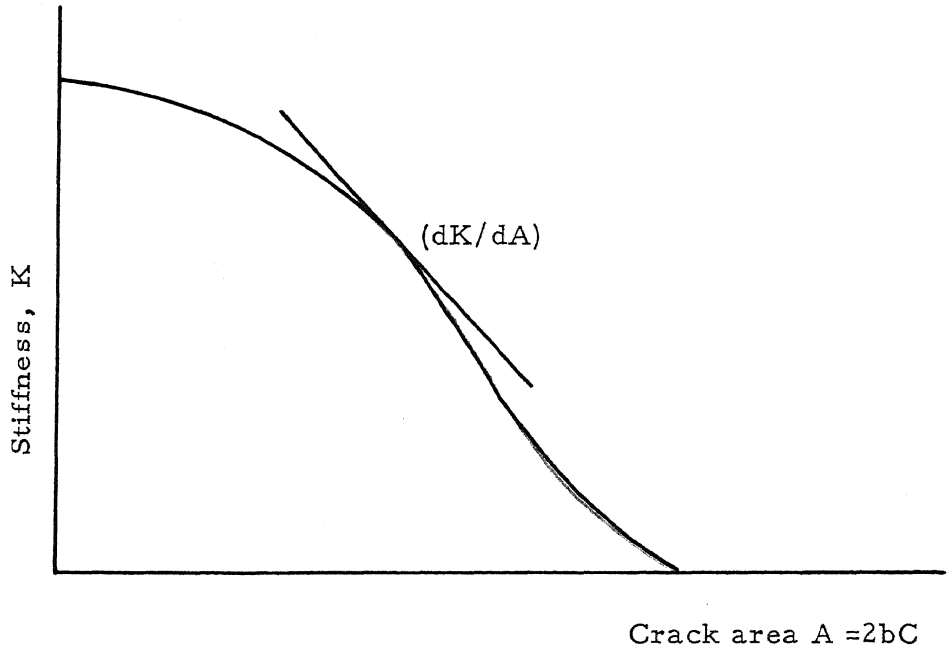

Figure 7. Curve of stiffness, K, versus crack area, A

III. EXPERIMENTATION

(I) Introduction:

In this experiment, the surface energy of plexiglas was obtained for a variety of specimen dimensions. The results were used in eight different equations for evaluating surface energy and a comparison made between the results to find which was the most reliable. The experiment was carried out in three parts.

The purpose of the first part was to develop experimental procedure and to evaluate the equations in conditions where specimen dimensions were changed but kept as constant multiples of each other. The second part was designed to show how the shape of the notch tip cut in the specimen affected the value found for the surface energy. The third part was sub-divided into two sections, in one of which the total specimen height was kept constant but the notch length varied, in the other, the uncracked height of the specimen was kept constant while the notch length was varied.

(II) Material, and Preparation of Specimen:

The material used was a plexiglas obtained commercially in various thicknesses. Specimen were prepared from the sheets to fit the required dimensions (Table IV) and where the thickness

required lay between supplied values, the required size was initially obtained by milling the specimen. In examining the fracture patterns obtained in the first part of the experimentation it was found that scratches left by the milling machine on the specimen were affecting the crack path and in the later part of the work the specimen dimensions were changed to be dependent on the original thickness of the plexiglas. The reasons for the selection of plexiglas were that it is optically clear and generally free from internal flaws, easy to work with and relatively inexpensive, and that it fractures easily along a plane allowing surface area to be measured easily.

It was necessary for the top and bottom specimen surfaces to be parallel and accordingly these two surfaces were ground, it was, however, found difficult to prepare a specimen to within a tolerance smaller than 0.05 inches to meet this requirement. Thus averaged values of the height were used for each group.

In the first part of the experiment, the notches were cut into the specimen using a lathe but this did not give satisfactory results since a slight curve to the notch tip was generated across the thickness of the specimen. While this has some use in crack growth control (10), the change in stress state thus created affected the results and accordingly a milling machine was used instead to give

a straight cut across the specimen.

In the initial experiment notches were cut with a V shaped tip and were dimensioned to be the same size relative to the specimen length for all cases. In the second experiment, three different shapes of notch, the square end U, the sharp V and the rounded end wire saw notch were used, but the crack length was kept in proportion to the basic specimen dimension, all specimens being cut to the same length; height: thickness ratio.

In the third experiment, the notches were cut to different depths of the specimen, which was kept at constant thickness and length. The experiment was carried out in two parts. In the initial part of the experiment the total height of the specimen was kept constant but crack length and tip shape were varied, using V, U and I type of notches. In the second part of the experiment, the thickness of the uncracked specimen was held constant while the notch cut length was changed, only V notches were used in this part of the work.

(III) Apparatus Used

Three components made up the experimental equipment:

1. Loading Stand: An overall view of the equipment used to apply load is given in Fig. 8, and a detail photograph of the

loading system in Fig. 9. Load was applied to the specimen manually by rotating the short bar at the top left of the frame, which turned the small toothed wheel below, which was meshed into the central geared drive wheel. This central wheel could be raised or lowered relative to the central loading rod in order to adjust to the different dimensions of the specimen. A bearing section was set below the central drive rod to remove the radial component of motion. A Kistler Model 912 Quartz load cell was positioned between the bearing section and the knife edge and allowed the load to be read from directly over the specimen. Two roller bearings, acted as point supports and were set on the base of the stand. Their position could be adjusted, so that the distance between them could be changed for the different specimen dimensions.

2. A dial indicator was positioned over the top of the loading rod to measure the central deflection of the beam, but this was very sensitive to relative movement around the working area (Fig. 9), accordingly in the third experiment, it was replaced by an LVDT, the core of which was attached to the bearing housing and the armature section to the support platform (Fig. 10). The LVDT read-out of load displacement was through a chart recorder.

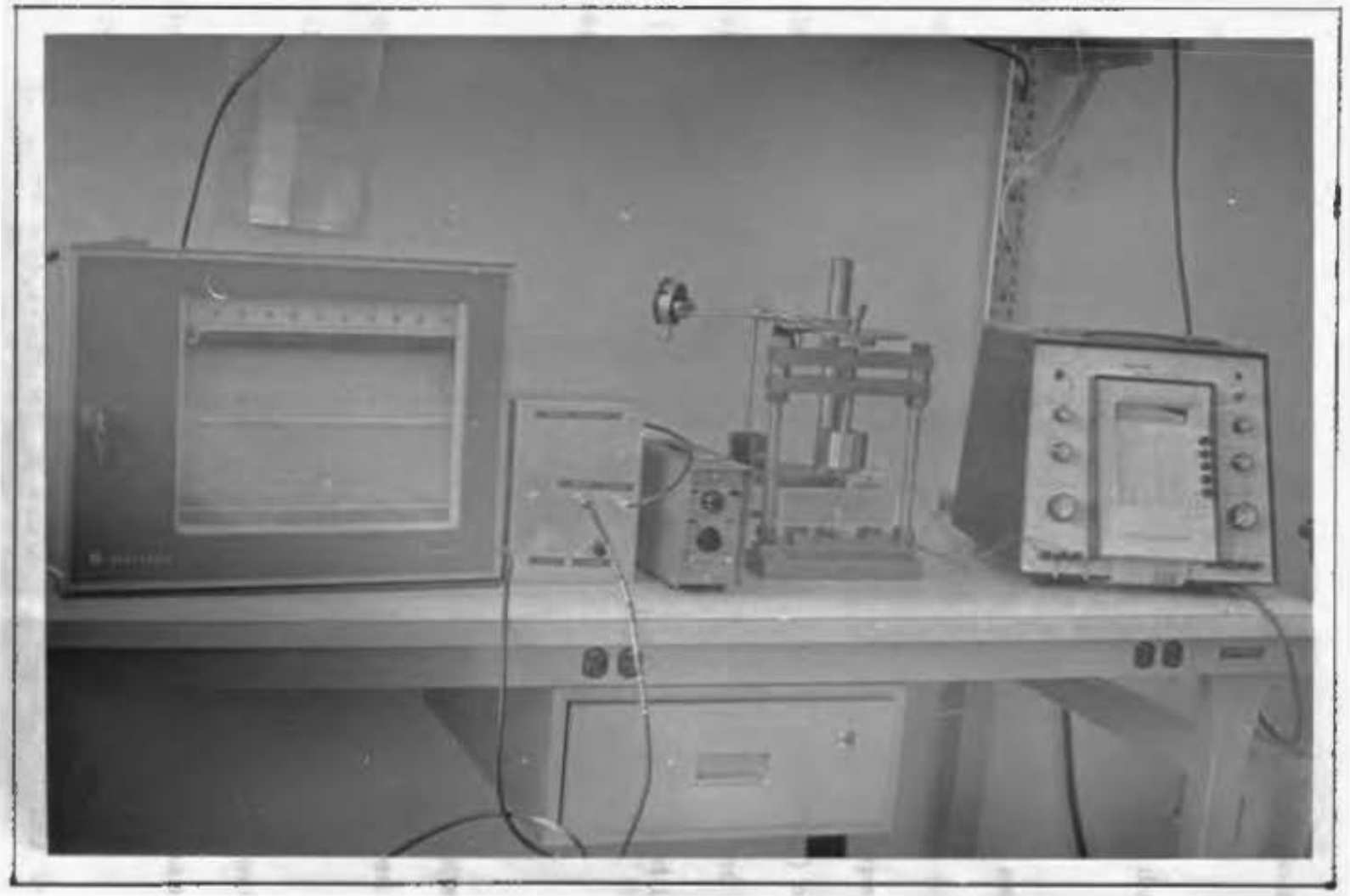

Figure 8. Experimental layout

(IV) Experiment Procedure

The procedure for testing the specimens in three point bending was :

1. Use a circular saw to cut the plexiglas into the desired dimensions.

2. Grind the specimens both top and bottom to the exact dimensions.

3. One of three kinds of notches was made in the specimen. In each specimen either a square end (U), sharp end (V) or a wire saw cut (I) was placed in the center and cut to a specified depth. The method of cutting the wire saw notch (I) is discussed in the appendix.

4. The specimens were loaded.

5. Deflection of the load for the first and second experiments was read from the dial gage at the time load was initiated on the specimen, and at the instant of crack propagation.

6. For the purpose of overcoming temperature effects the load cell, being responsive to the heat of the operators hand, was covered with 3140 RTV coating.

7. Care was exercised in centering the specimens in the loading stand, and the load was applied at a low and constant rate to permit

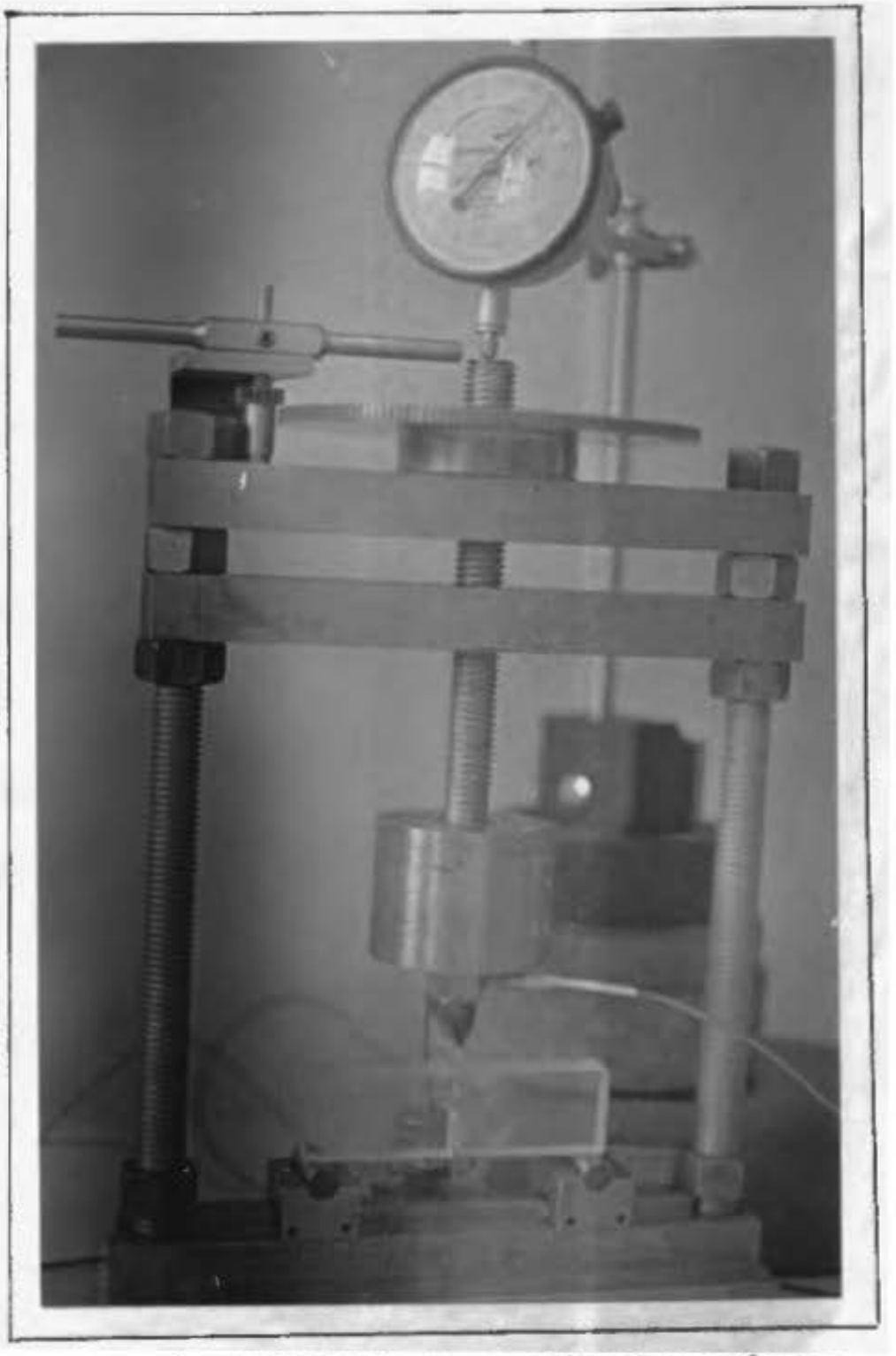

Figure 9. A Dial Indicator positioned over the top of the loading rod.

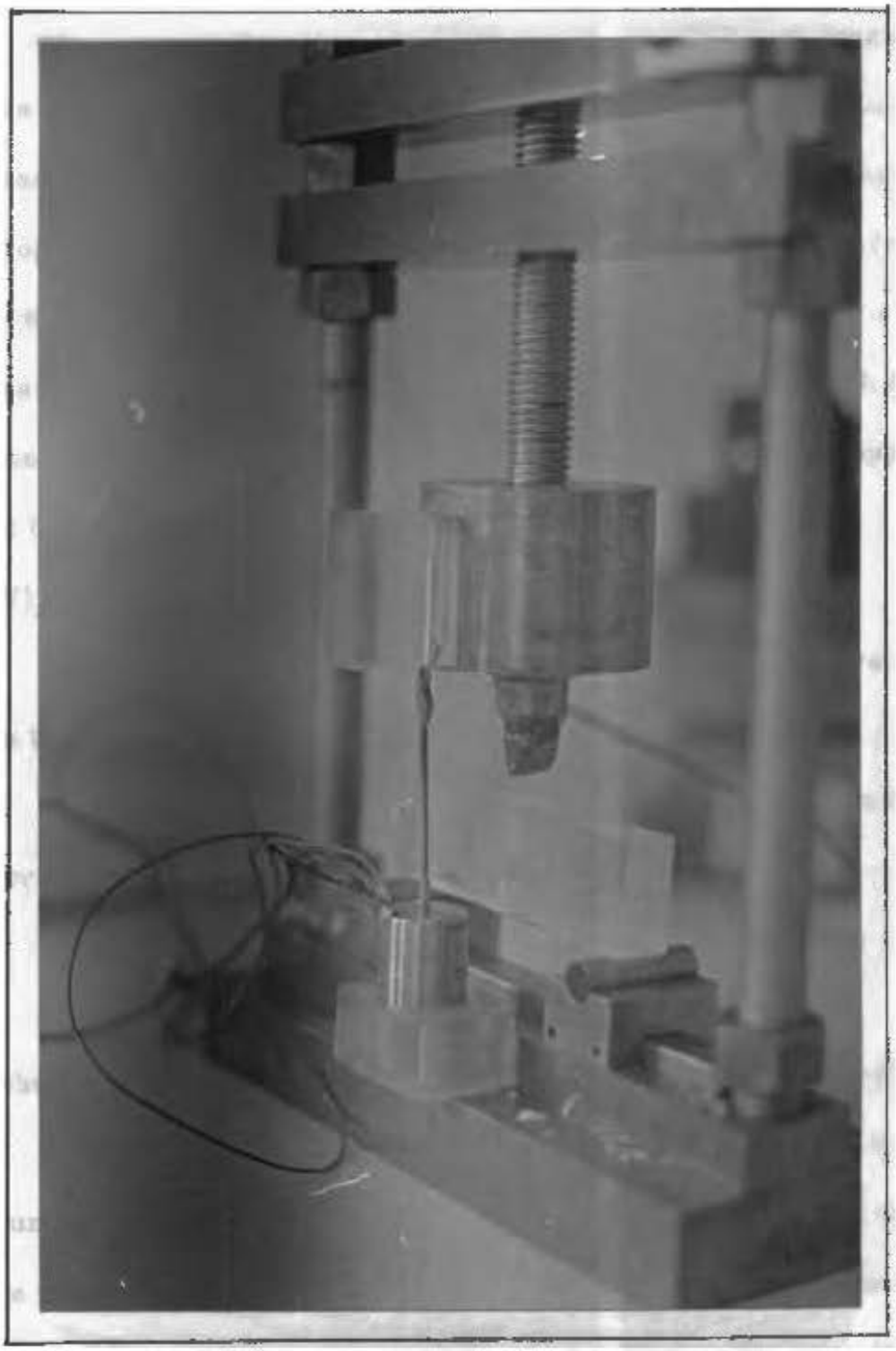

Figure 10. An LVDT attached to the bearing housing and the armature section to the support platform

adjustment of the on-load point.

8. To prevent the crack from running the entire length of the specimen it was necessary to give particular attention to the load application, keeping the loading rate slow and constant and stopping at the instant the crack started to grow. It was found better to observe this initiation by watching the recorder since the load began to drop off before any visible crack growth has occured giving warning and allowing the loading to be stopped at the correct time.

(V) Analysis of the Results and Discussion

The assumption upon which all the equations used are based in that the Griffith theory of crack propagation holds.

For this to be true Rose and English (17) have shown that, for geometrically similar beams, the relationship

$$\frac{P^2}{D^3} = \text{constant}$$

where P is the applied load and D is a specimen dimension.

In the equations cited this constant has been related to the surface energy of the material, so that, for the equation used to be valid, the surface energy value obtained should be constant.

The numerical results of the experiments are given in the appendix and graphically represented in Fig. 11 to Fig. 16.

Taking these in turn, the two effective surface energy values are compared with those obtained by the various mathematical equations (given as equations III-VIII), and those equations which do not give a constant value for suface energy are considered invalid. Fig. 11 to Fig. 13 show surface energy values, obtained using all eight equations, plotted against crack length. It can be seen Fig. 11 that the curves for equation III and equation VII do not give a constant values for surface energy and so are probably invalid, and have accordingly been neglected in favour of the other equations from hereon.

For the same reason since the graph given in Fig. 13 indicates that all the equations give sensibly constant values except equation VIII, for which the surface energy apparently varied in proportion to the crack length this equation too is considered incorrect. The remaining equations are plotted in Fig. 14 to Fig. 16 against the crack penetration ratio. The theoretical equations give sensibly constant values but equation I is no longer considered because of the qualifying assumptions made to creat it and equation II is considered the effective value, since it takes into consideration the residual energy stored in the specimen after fracture.

Fig. 17, 18, 19 plot surface energy versus uncracked beam height for equation II, equation IV, equation V and equation VI

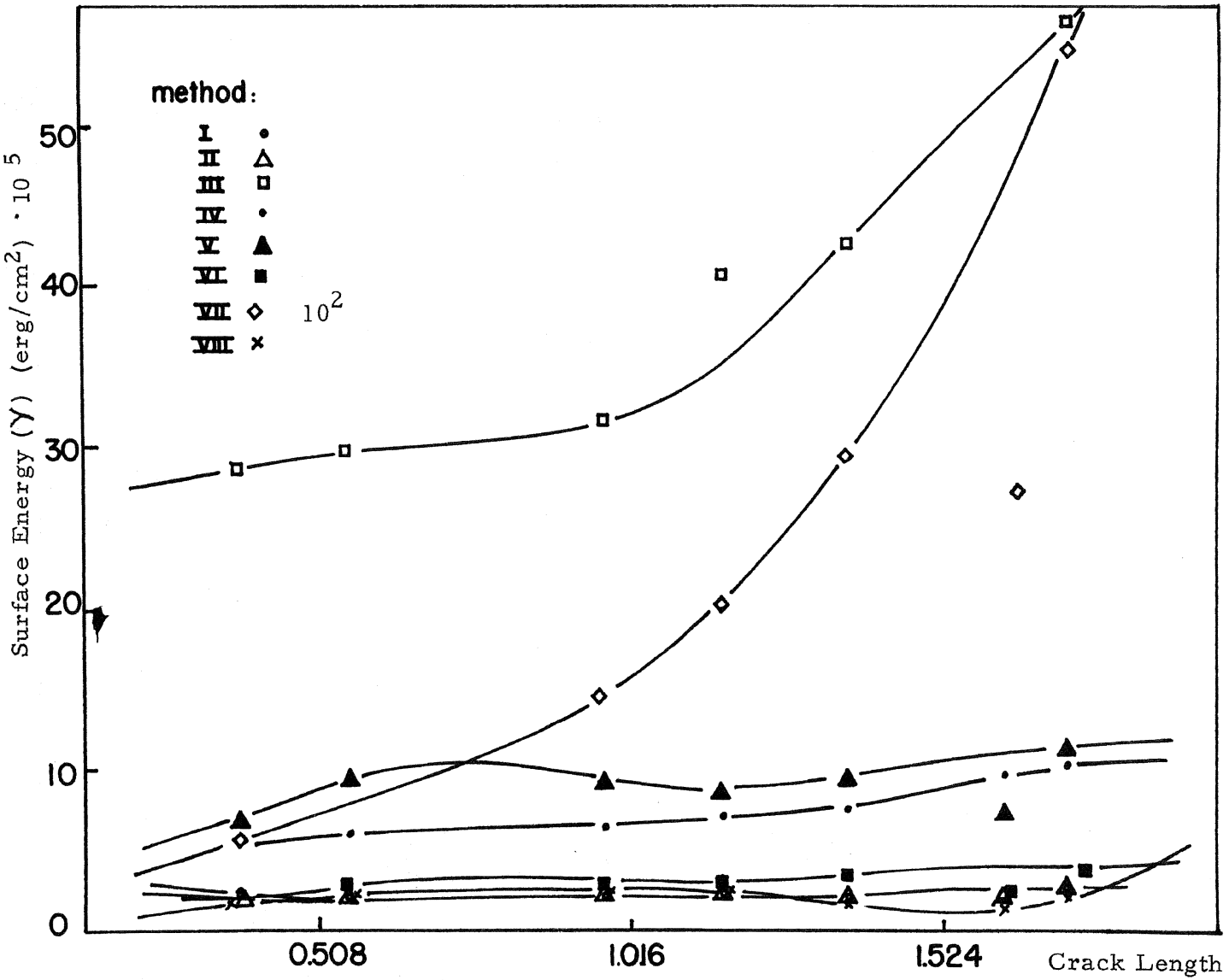

Figure 11. Surface Energy (γ) plotted against Crack Length (C) for Group I

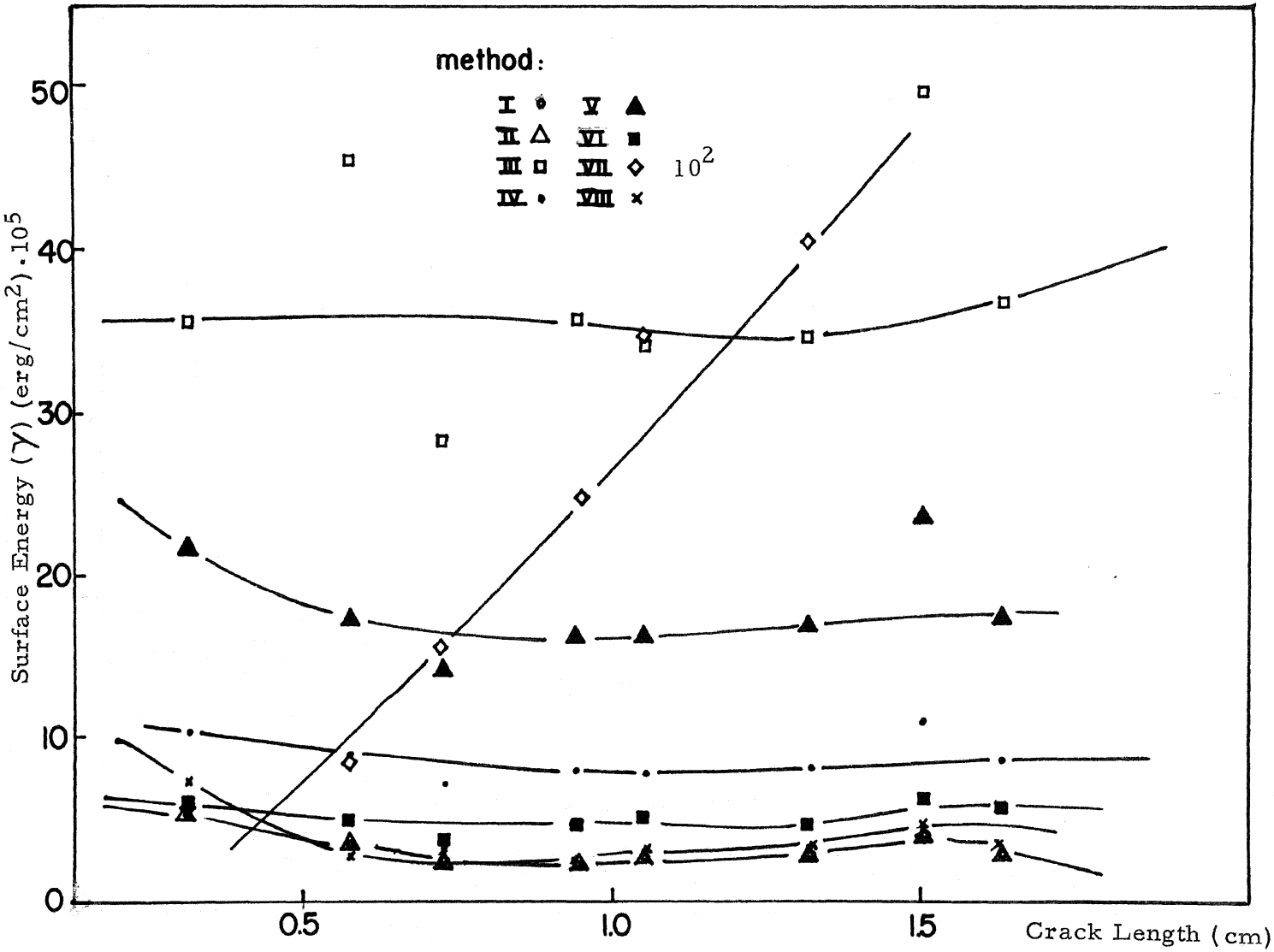

Figure 12. Surface Energy (γ) plotted against Crack Length (C) for Group II

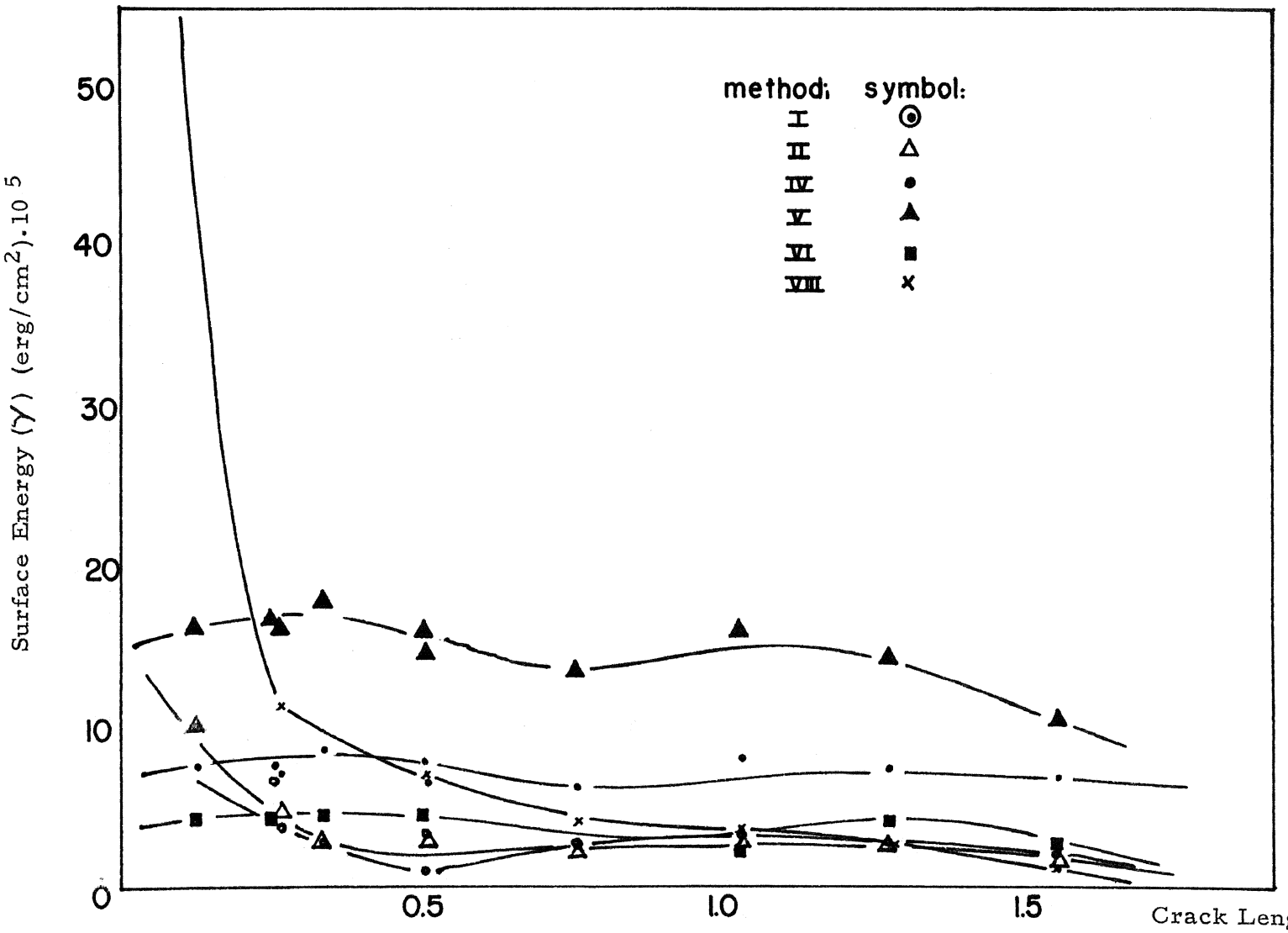

Figure 13. Surface Energy (γ) plotted against Crack Length (C) for Group III

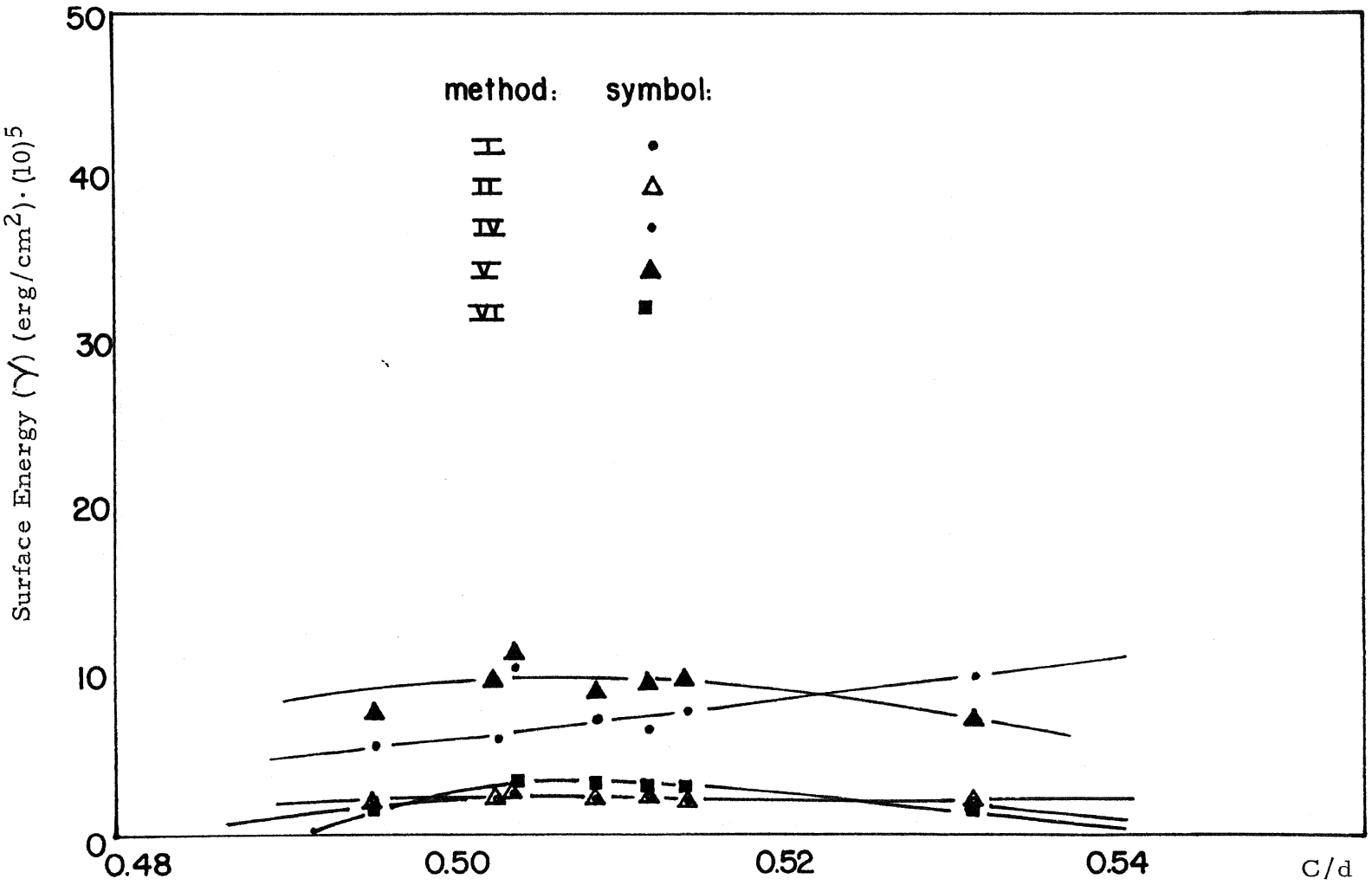

Figure 14. Surface Energy (γ) plotted against Penetration Ratio (C/d) for Group I

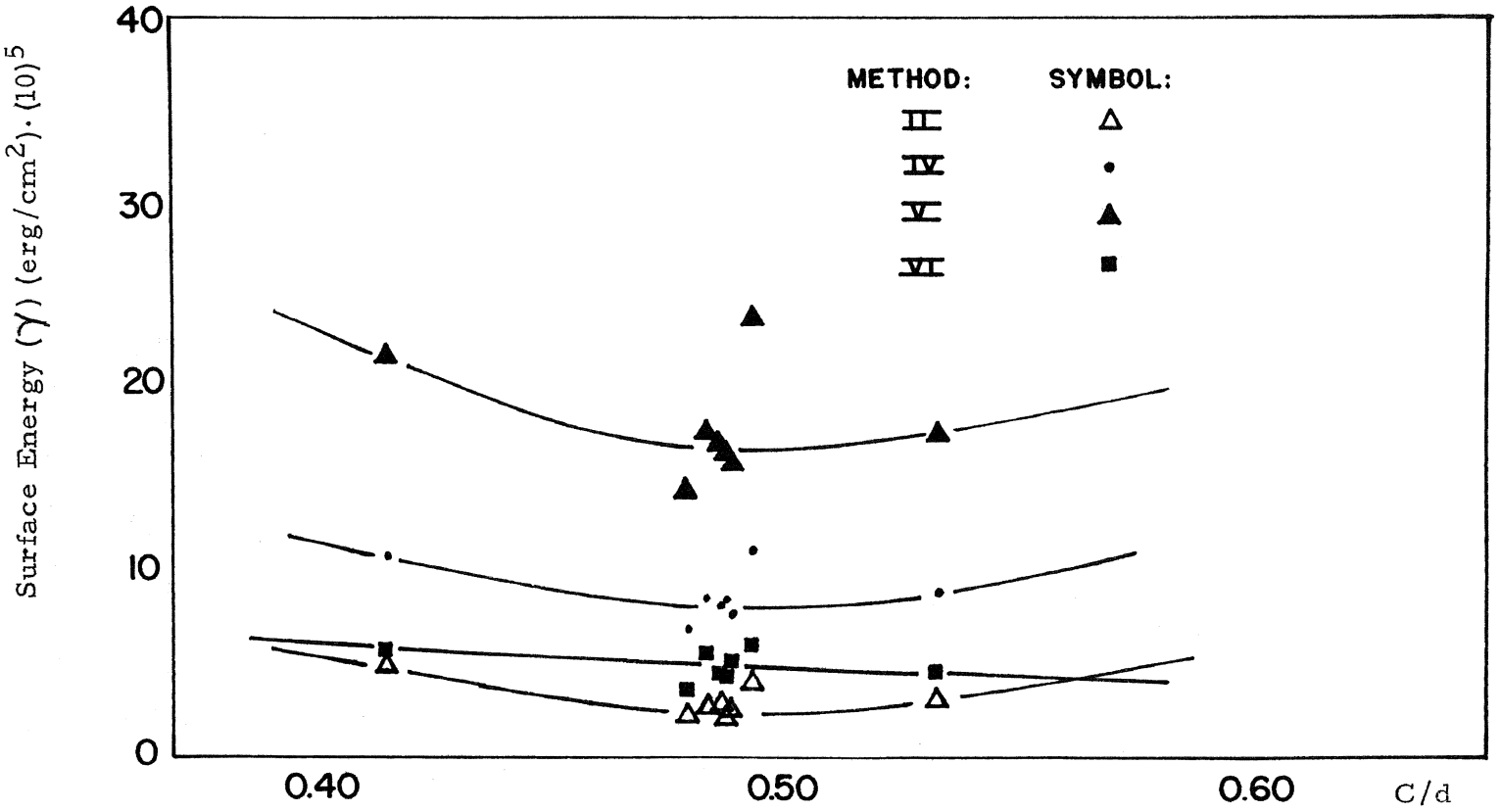

Figure 15. Surface Energy (γ) plotted against Penetration Ratio (C/d) for Group II

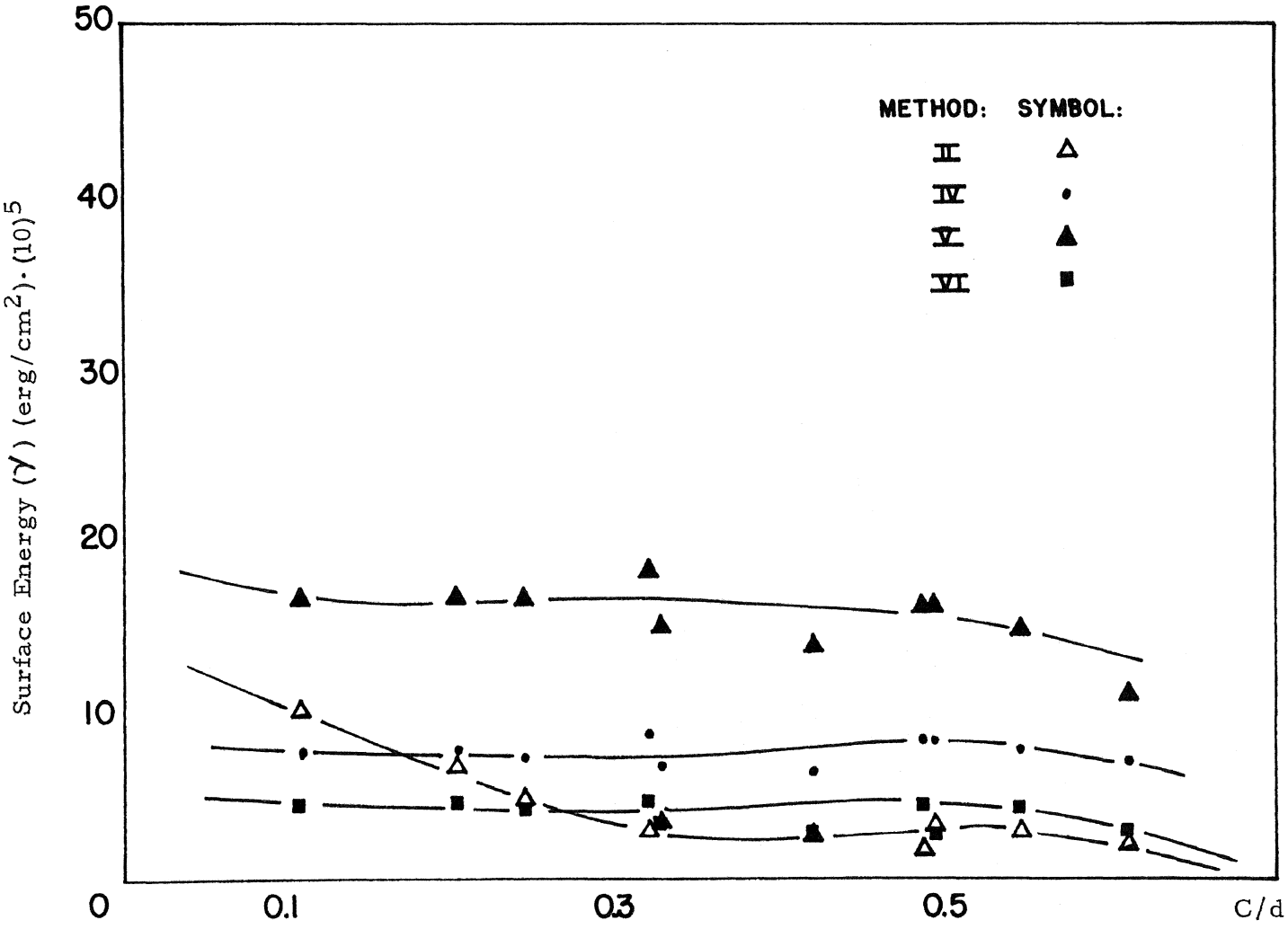

Figure 16. Surface Energy (γ) plotted against Penetration Ratio (C/d) for Group III

Fig. 17 indicates an increase in surface energy with uncracked height for equation IV, and equation V, and for this reason, these equations would appear incorrect. Fig. 19 indicates a change in surface energy value with a variation in uncracked beam height. It illustrates that equation VI gives a constant value for surface energy, but equation II indicates that the values of surface energy vary with uncracked beam height, thus equation VI would seen more reliable than equation II. The result of this analysis is to leave one effective surface energy evaluation (equation II) and one theoretical (equation VI) which are shown in Fig. 18 and Fig. 19 respectively. The most reliable of the theoretical equations for effective surface energy determination would be equation VI. Further discussion of these points is made in the next chapter.

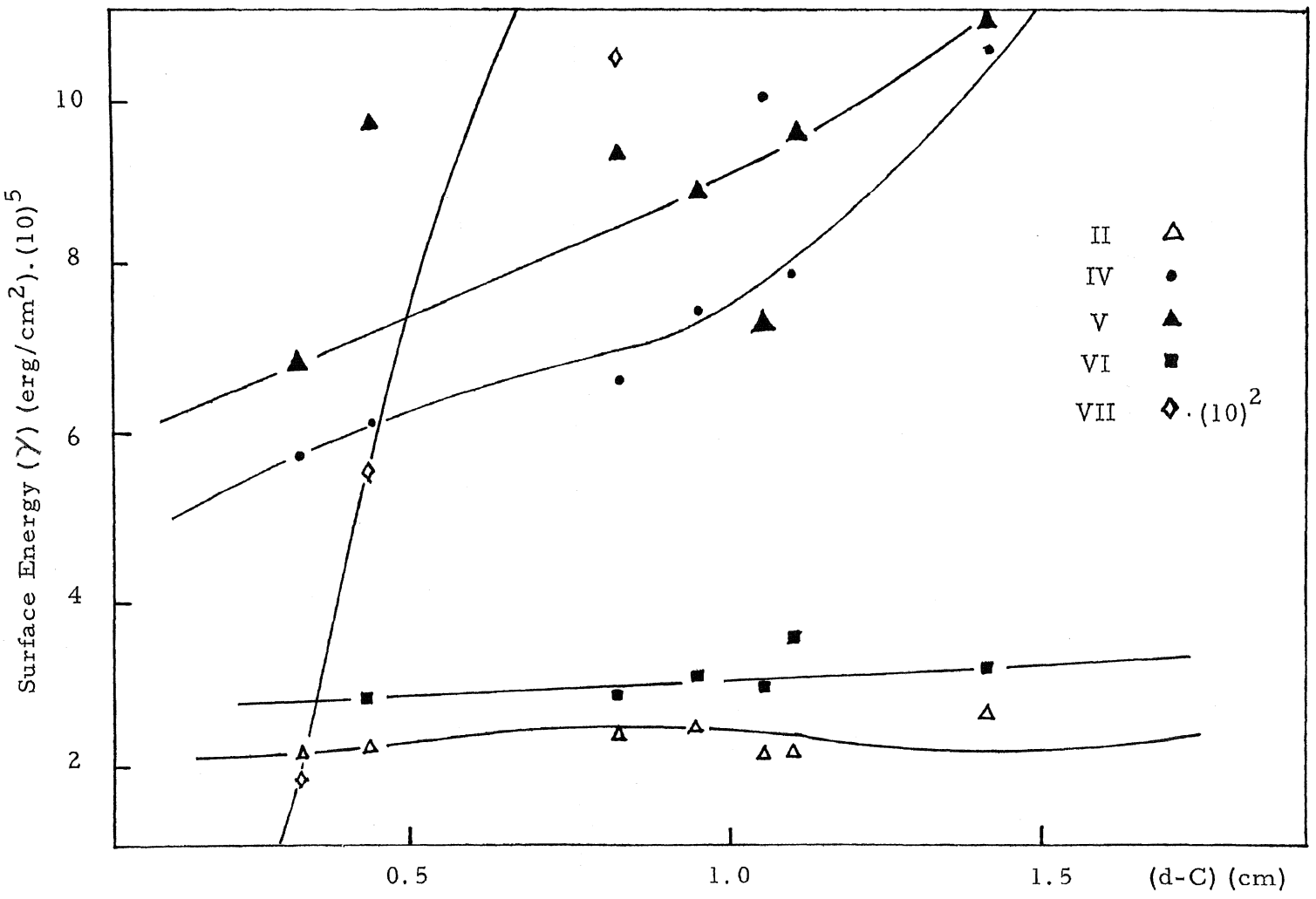

Figure 17. Surface Energy plotted against Uncracked Beam Height (d-C) for Group I.

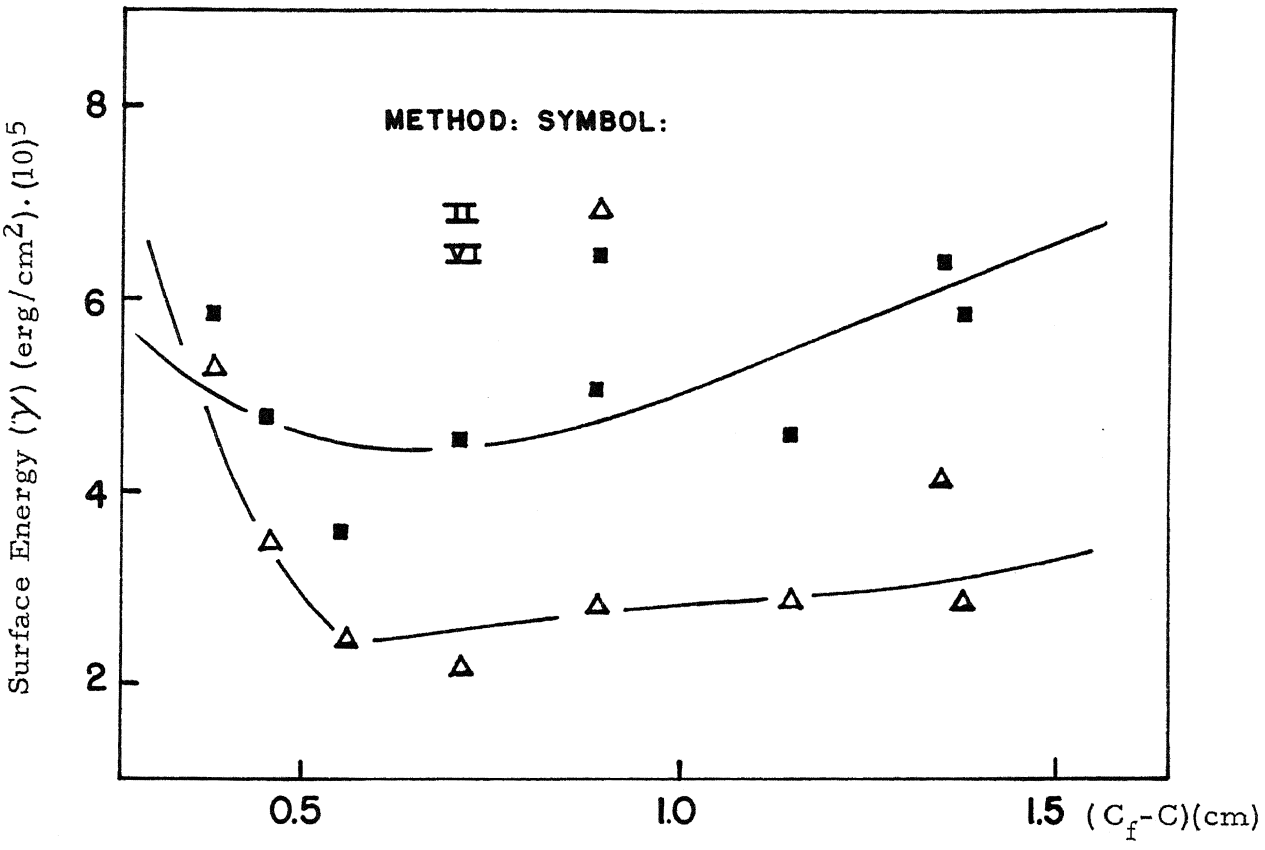

Figure 18. Surface Energy (γ) plotted against Crack Extension (C_f - C) for Group II

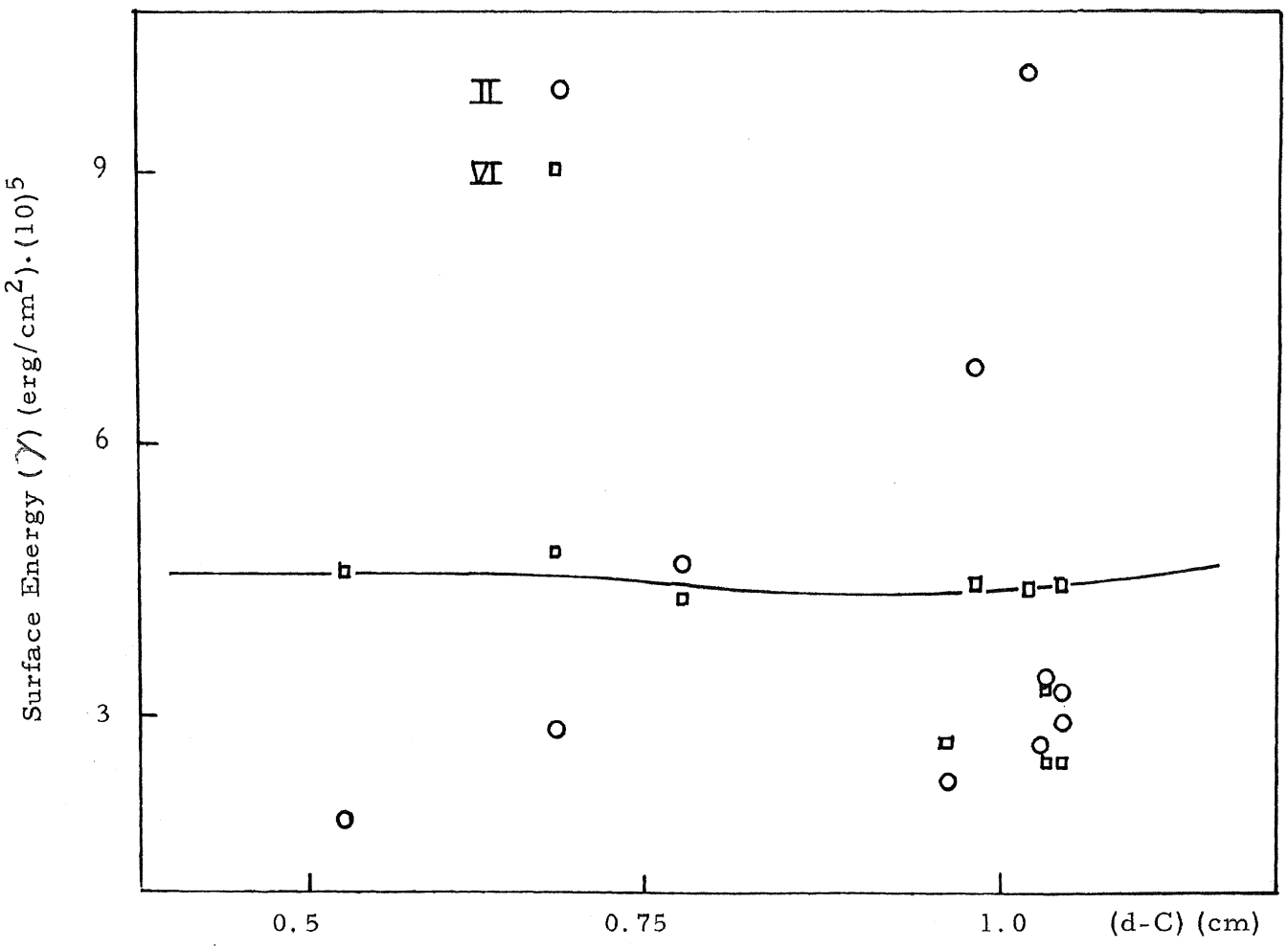

Figure 19. Surface Energy (γ) plotted against Uncracked Beam Height (d-C) for Group III.

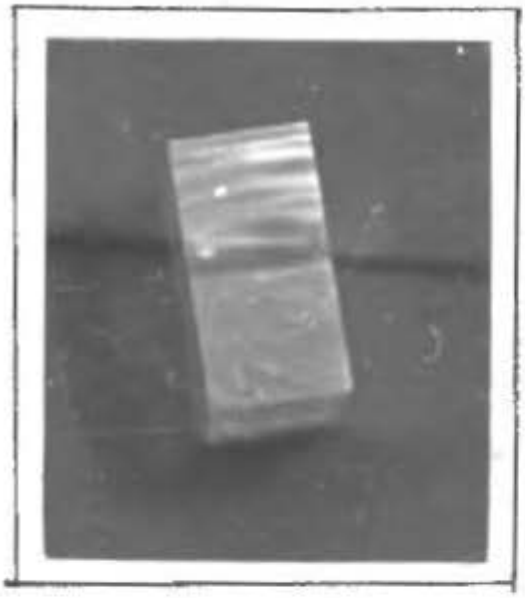

Figure 21. Mirror finish to crack surface

Figure 20. River line finish to crack surface

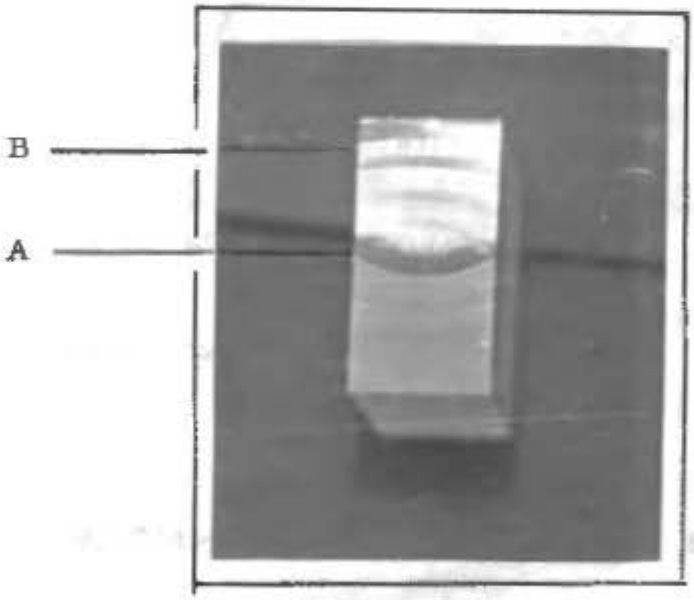

Figure 22. Crack surface showing velocity transition points (A and B)

IV. ANALYSIS OF RESEARCH, CONCLUSIONS AND DISCUSSION OF FURTHER WORK REQUIRED

(I) The Validity of the Griffith Theory and an Equation for calculating Surface Energy of a Material

Rose and English (17) have shown, using the theory of dimensions, that for the Griffith theory to be valid the relationship

$$\frac{P^2}{D^3} = \text{constant}$$

must hold, for specimens of constant dimensional proportion. As all the theoretical equations used are based on the Griffith theory, they also are reduceable to this relationship which can be arranged so that the constant is given as the surface energy of the material. For example Srawleys equation

$$\gamma = \frac{9\,P^2L^2C}{8\,Eb^2\,d^4}\,(A_o + A_1(C/d) + A_2(C/d)^2 + A_3(C/d)^3 + A_4(C/d)^4)^2$$

can be reduced to

$$\gamma = \frac{P^2}{d^3} \cdot \text{constant}$$

where L/d, C/d and L/b are held constant. Examination of the data indicates that, of the equations examined, only the above equation yields a constant value for surface energy for the results

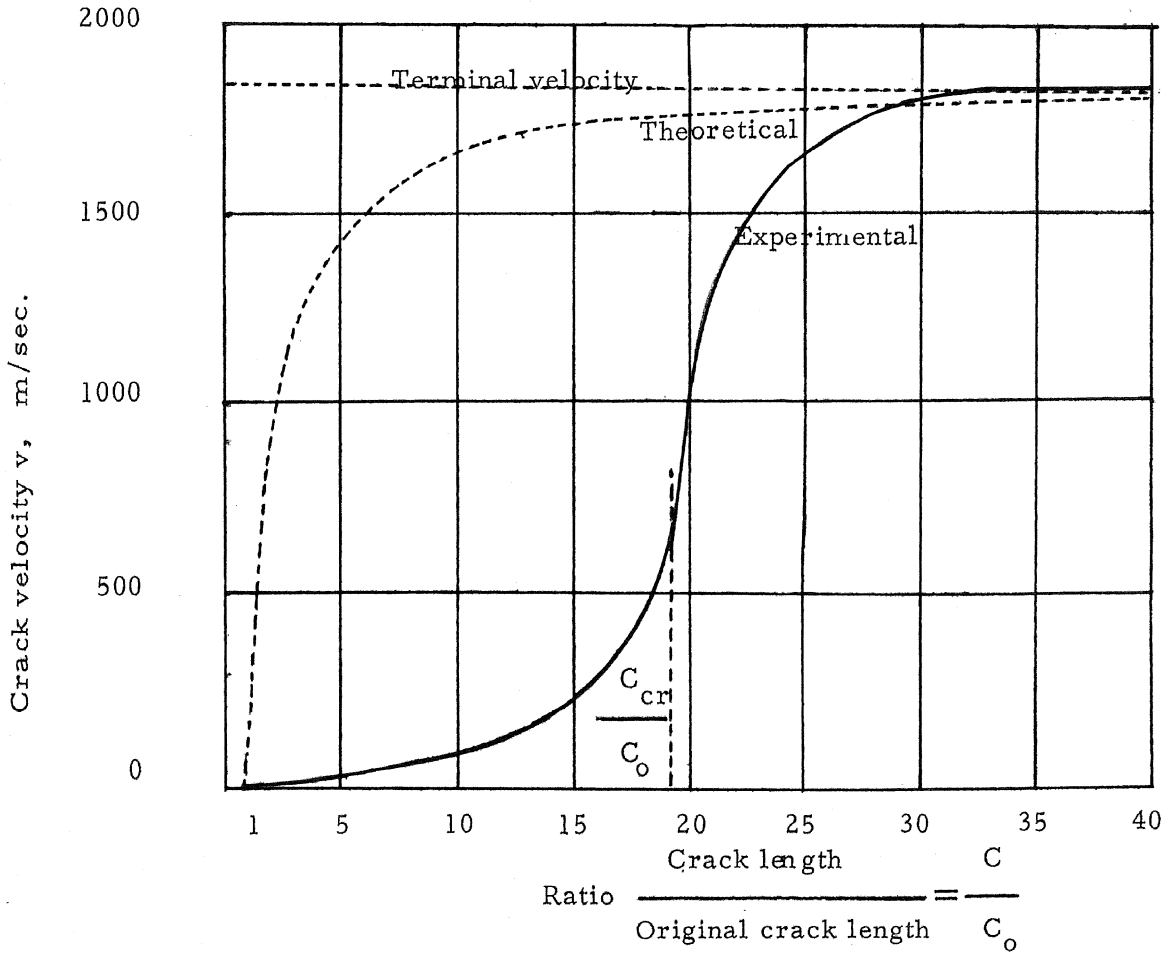

Figure 23. Crack velocity related to crack length (after Bieniawski (18))

obtained from the experiments. Srawley's equation therefore will yield data which verify that the Griffith theory holds. As the other equations do not do this, then they are not valid in the present case.

(II) The Bieniawski crack velocity criterion

Bieniawski (18) has stated that crack propagation can be divided into two types, namely stable and unstable. Stable propagation is defined as the failure process of fracture propagation in which the crack extension is relatively slow and a function of the loading and can be controlled accordingly, and unstable is defined as the failure process of fracture propagation in which the crack extension is also governed by factors other than the loading, and thus becomes uncontrollable. Both of the above phenomena were observed during the series of tests carried out. Stable growth was characterized by well defined (Fig. 20) river lines while the unstable showed a clear mirror finish (Fig. 21).

According to Bieniawski (18) the criterion which controls transition from stable to unstable crack propagation is a crack growth to about twenty times the original crack length, or in this case notch length (Fig. 23). This criterion was not found to hold true in all cases from the surface features observed in the specimens.

In some cases it was found that the mirror finish began very

close to the notch tip (Fig. 22) and in other cases (Fig. 20) the crack grew right through the specimen at a slow rate, indicated by the presence of the river lines.

The change in crack surface pattern found to occur in the specimens was marked by a rapid acceleration of the crack similar to that, described by Bieniawski (18), Schardin (19) and Wiederhorn (20) as the acceleration to terminal velocity, and a mirror finish to the crack surface is accordingly taken as an indication that terminal velocity has been reached. As this was found to occur in a number of specimens almost at the root of the crack (Fig. 22) the Bieniawski criteron can not be said to hold for plexiglas specimens failing in flexure.

(III) The effect of notch size and shape on the results obtained

The effects of three different shapes for the notch type were examined in the experimental work, square, sharp V and rounded. Of these three, the V tip consistently gave the lowest value for the surface energy. There was no consistency in the variation in results obtained with the two other shapes and all three shapes produced results of approximately the same value.

The importance of the depth of the notch was found to be related to the penetration ratio (depth relative to that of the specimen) rather than to the notch depth as an absolute value. Where the pene-

tration ratio was less than 0.3 the crack frequently grew completely through the specimen and values calculated for surface energy using the area created (equation II) gave artificially high values, since this does not consider the energy still stored in the specimen at the time of total failure. This inaccuracy does not occur in the Srawley equation, which considers only the parameters at the time of crack initiation.

On the basis of the experimental evidence of this investigation, the following conclusions were drawn.

1. Graphical analysis of the results indicated that the Srawley's equation is valid for obtaining surface energy values, where values of the 'A' terms are related to the length: height ratio, and gives a sensibly constant value for surface energy calculation.

2. The effect of varied notch shape on crack initiation load for different crack length did not indicate much difference between the shapes, as shown in Figure 33 although in some cases the curve did not give a sensibly constant value, the reason being that the procedure used to obtain the round (wire saw) notch was very difficult to perform. Especially it was found difficult to obtain the desired dimension and to keep the notch straight and for this reason round notches were not cut to a uniform depth, which caused surface energy values calculated for crack extension to vary slightly.

3. The Bieniawski criterion for crack velocity control does not hold for plexiglas in flexure.

4. The Griffith criterion for fracture extension is satisfied, even where the initiating crack is over 1/2 inch long.

5. Crack shape is important only where the width of the notch becomes relatively large (of the order of 0.05").

In the area of recommended future work a more detailed study of the fracture surface is suggested, since there were many features observed the causes of which are presently unknown. High speed photographic studies are also recommended to observe the transition from slow to rapid crack propagation. The validity of the Srawley equation for determining the surface energy of rocks should be further investigated.

Figure 24. Fracture surface indicating hair-like discontinuities

Figure 25. Fracture surface for different types of notch shapes

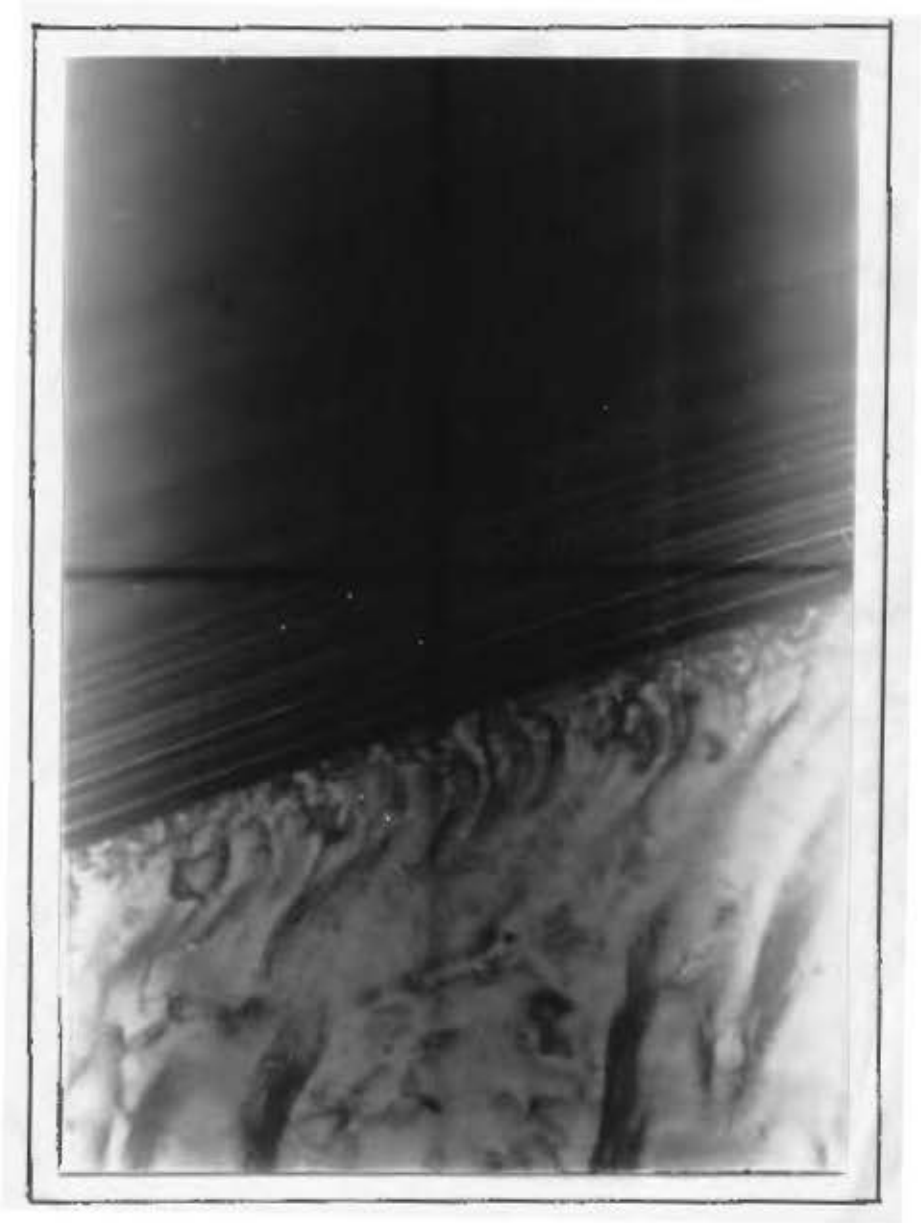

Figure 26. Crack initiation surface showing initial ductile fracture

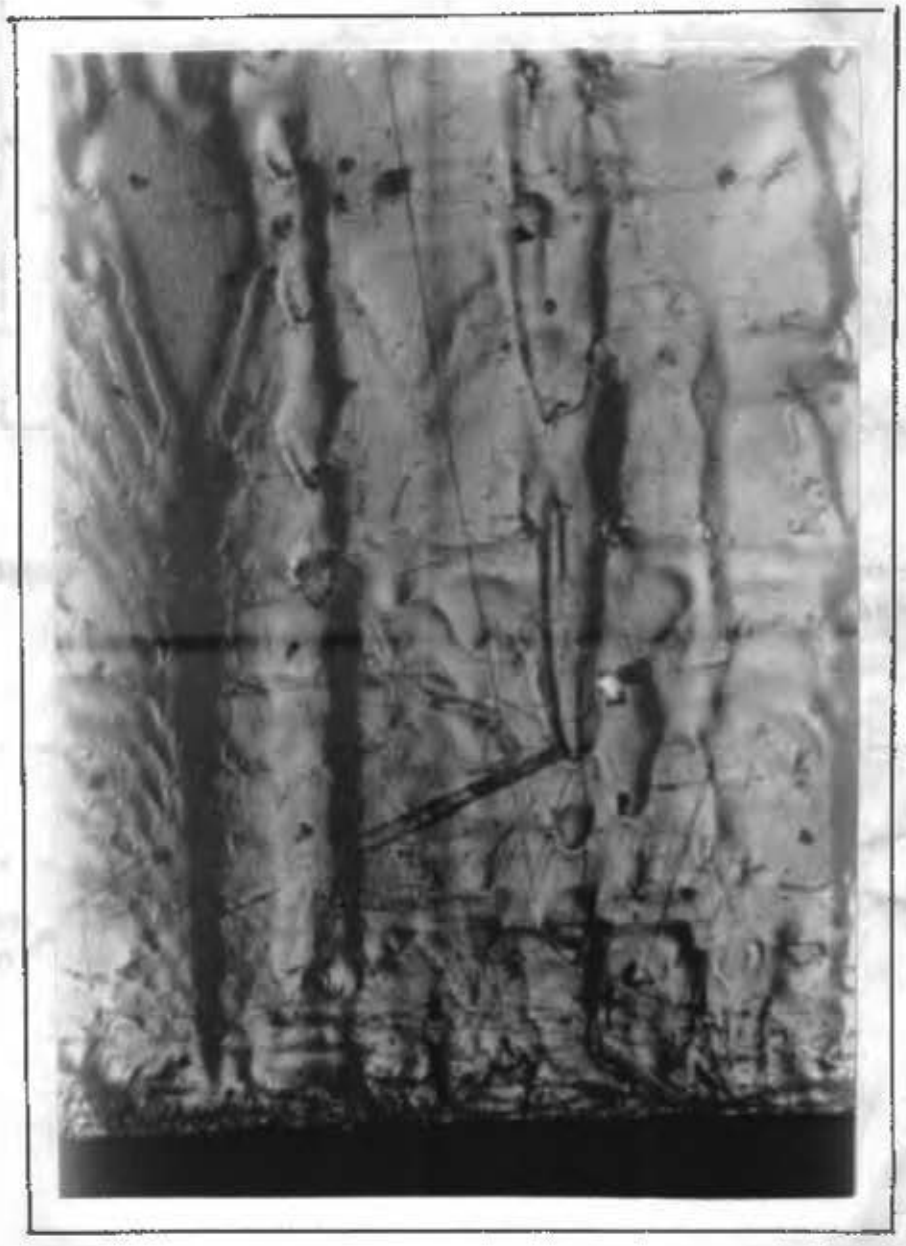

Figure 27. Fracture surface showing chevron effect (crack growth from the top of the page)

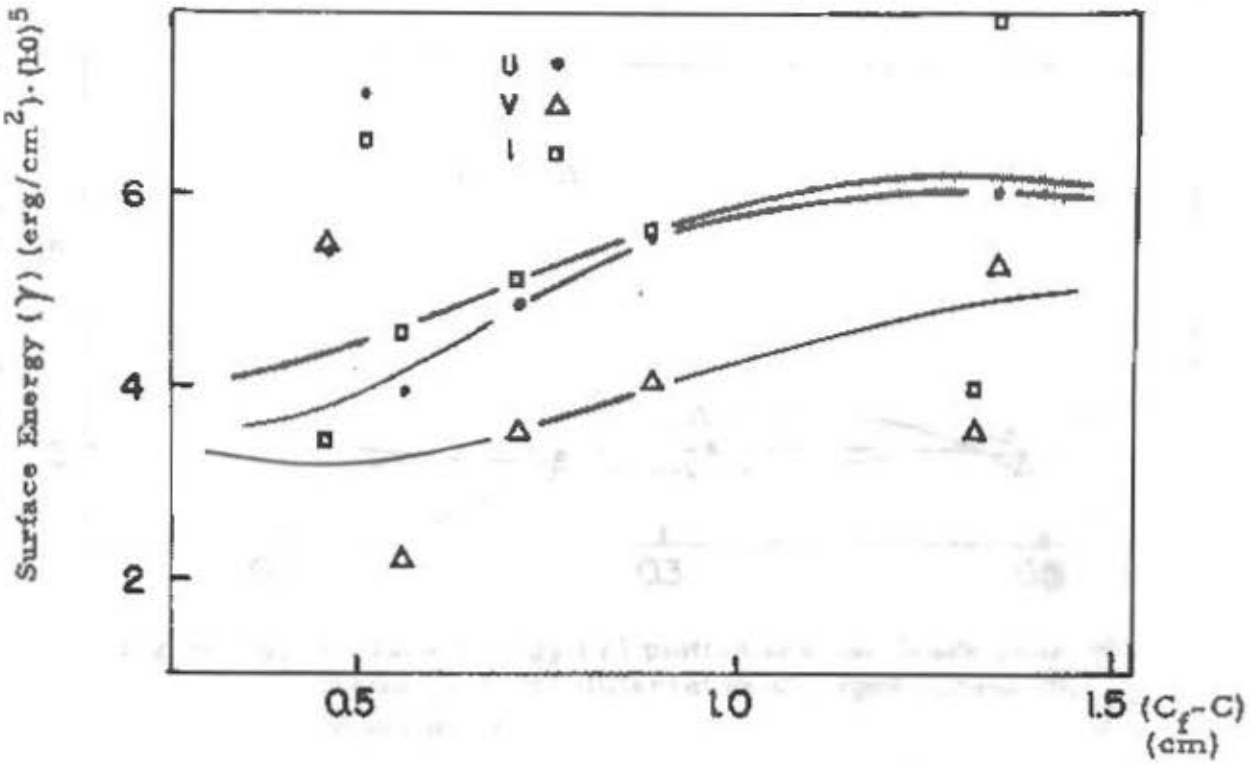

Figure 28. Surface Energy (γ) plotted against Crack Extension for different notch types (Group II, equation VI.)

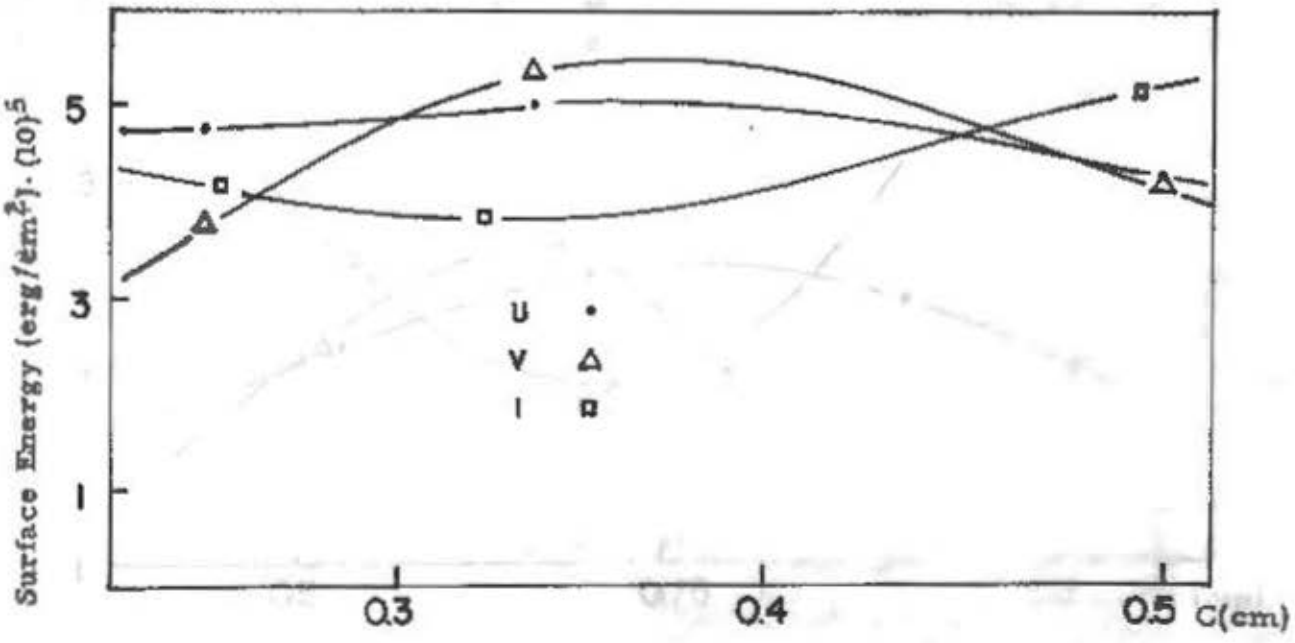

Figure 29. Surface Energy (γ) plotted against Crack Length(C) for different notch types (Group III, equation VI.)

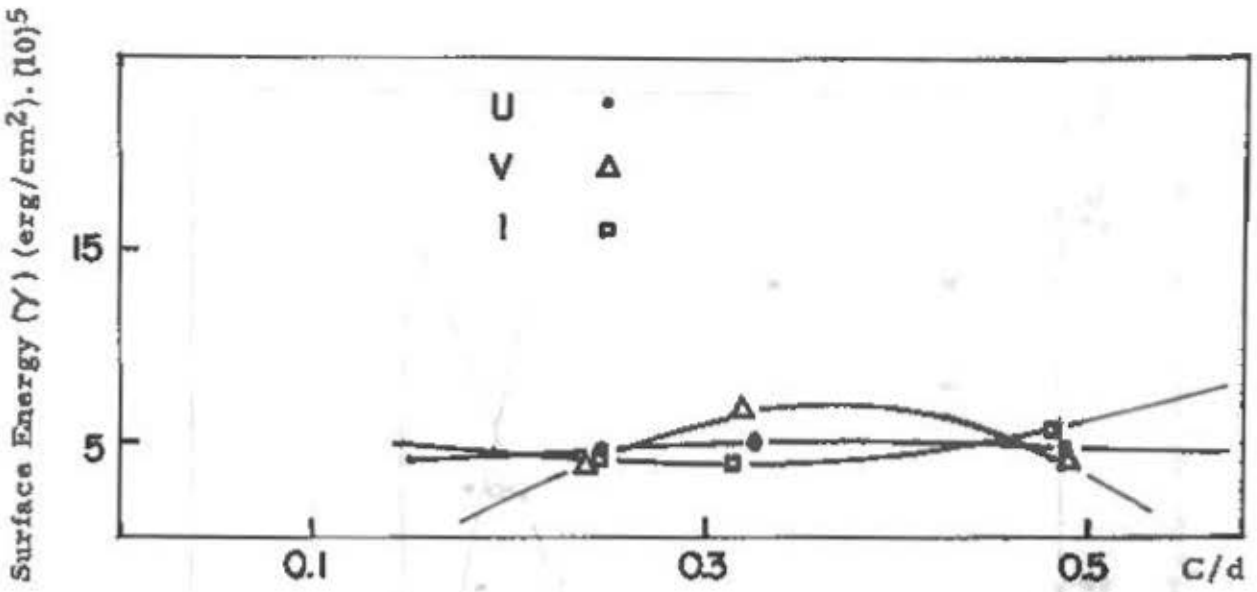

Figure 30. Surface Energy (γ) plotted against Crack Penetration Ratio (C/d) for different notch types (Group III, equation VI.).

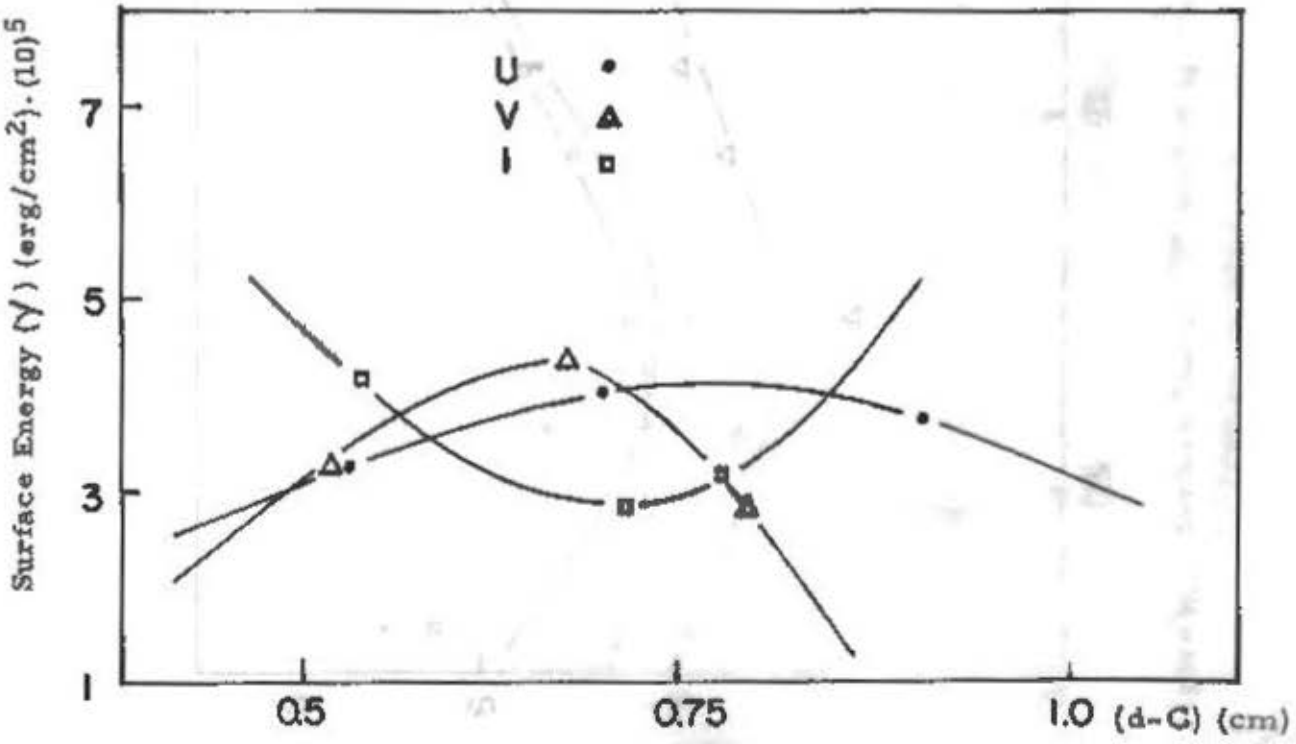

Figure 31. Surface Energy (γ) plotted against Uncracked Beam Height (d-C) for different notch types (Group III, equation VI.).

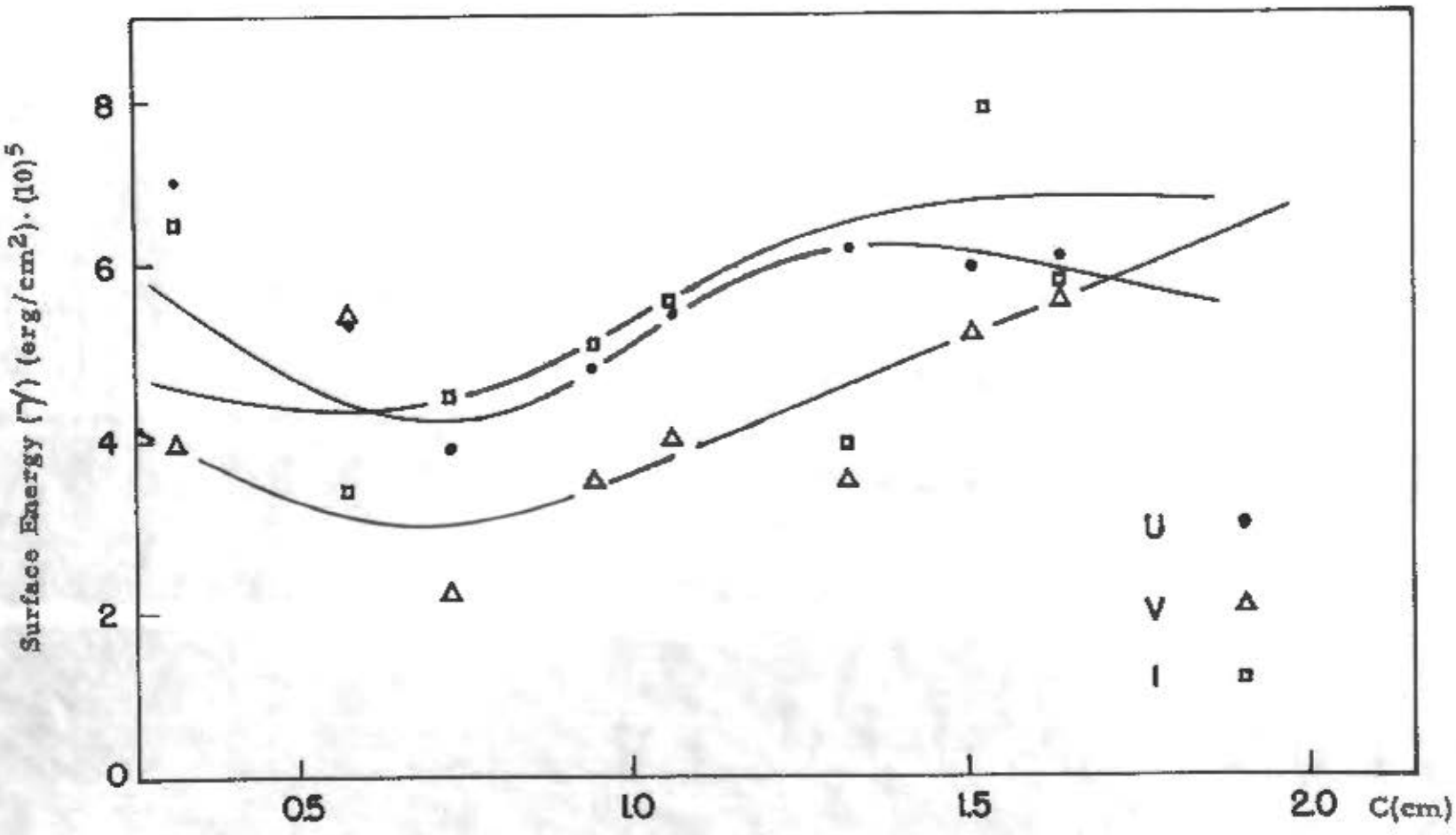

Figure 32. Surface Energy (γ) plotted against Crack Length (C) for different notch types (Group II, Equation VI.)

Figure 33. Crack growth for different notch shapes

V. APPENDICES

(I) Appendix I.

This appendix gives a list of Tables representing the data and results for each specimen.

TABLE IV.

DATA FOR SPECIMEN USED(GROUP I)

No. of Specimen	Height d (inch)	Original Crack C (inch)	Uncracked Height d-C (C_f-C) (inch)	Penetration Ratio C/d	Distance between Supports L (inch)	Max. Load P (lb)	Residual Load P_r (lb)	Displacement δ (inch)
1-a	0.295	0.145	0.130	0.4746	0.960	8.520	0.29	0.0110
1-b	0.298	0.14	0.120	0.4698	"	8.820	0.588	0.0087
1-c	0.300	0.16	0.120	0.5333	"	10.00	0.2941	0.0108
1-d	0.300	0.15	0.150	0.5000	"	9.704	0.147	0.0087
1-e	0.300	0.15	0.120	0.5000	"	10.00	0.294	0.1050
Average	0.298	0.15	0.120	0.4955	0.960	9.409		0.0098
Thickness (b) =0.15 inches								
2-a	0.42	0.22	0.195	0.5238	1.44	20.59	0.0	0.0098
2-b	0.44	0.23	0.195	0.5227	1.44	18.38	0.0	0.0111
2-c	0.45	0.22	0.21	0.4889	1.44	20.59	0.0	0.0135
2-d	0.456	0.22	0.22	0.4824	1.44	19.12	0.0	0.0129
2-e	0.445	0.22	0.19	0.4943	1.44	19.12	0.0	0.0108
Average		0.22	0.202	0.5024	1.44	19.54	0.0	0.0115
Thickness (b) =0.224 inches								
3-a	0.606	0.295	0.311		1.92	35.2	0.0	0.0176

TABLE IV. (GROUP I continued)

3-b	0.600	0.300	0.300		1.92	33.82	0.0	0.0161
3-c	0.600	0.300	0.300		1.92	32.35	0.0	0.0160
3-d	0.600	0.300	0.300		1.92	35.29	0.0	0.0167
3-e	0.601	0.300	0.300		1.92	29.70	0.0	0.0177
Average	0.601	0.300	0.300		1.92			
Thickness (b) =0.30 inches								
4-a	0.748	0.400	0.300	0.5348	2.40	37.35	0.0	0.0129
4-b	0.75	0.375	0.370	0.5000	2.40	47.65	0.0	0.0186
4-c	0.746	0.380	0.330	0.5094	2.40	44.71	0.0	0.0178
4-d	0.747	0.380	0.330	0.5087	2.40	43.38	0.0	0.0176
4-e	0.75	0.380	0.300	0.5067	2.40	38.24	0.0	0.0129
Average		0.383	0.320	0.5119	2.40	42.27	0.0	0.0159
Thickness (b) = 0.377 inches								
5-a	0.90	0.500	0.320	0.5556	2.88	44.71	0.0	0.0156
5-b	0.90	0.450	0.360	0.5000	2.88	55.88	0.0	0.0156
5-c	0.901	0.450	0.40	0.4994	2.88	61.76	0.0	0.0213
5-d	0.900	0.46	0.345	0.5111	2.88	45.59	0.0	0.0139
5-e	0.902	0.44	0.355	0.4878	2.88	51.47	0.0	0.0128
Average		0.46	0.37	0.5089	2.88	54.60	0.0	0.0172
Thickness (b) = 0.452 inches								
6-a	1.04	0.54	0.44	0.5129	3.36	73.53	0.0	0.0168
6-b	1.05	0.535	0.43	0.5095	3.36	70.59	0.0	0.0160
6-c	1.05	0.54	0.45	0.5143	3.36	73 53	0.0	0.0171
6-d	1.05	0.54	0.42	0.5143	3.36	68.24	0.0	0.0153
6-e	1.05	0.54	0.425	0.5143	3.36	67.64	0.0	0.0152

TABLE IV. (GROUP I continued)

Average		0.54	0.43	0.5143	3.36	70.71	0.0	0.0161
Thickness (b)= 0.528 inches								
7-a	1.20	0.64	0.44	0.5333	3.84	74.71	0.0	0.0178
7-b	1.20	0.64	0.38	0.6333	3.84	73.53	0.0	0.0153
7-c	1.20	0.63	0.43	0.5250	3.84	74.12	0.0	0.0164
7-d	1.20	0.64	0.40	0.5333	3.84	73.53	0.0	0.0170
7-e	1.20	0.64	0.40	0.5333	3.84	68.24	0.0	0.0157
Average		0.64	0.41	0.5316	3.84	72.83	0.0	0.0164
Thickness (b) =0.604 inches								
8-a	1.35	0.69	0.55	0.5111	4.32	111.76	0.0	0.0197
8-b	1.35	0.68	0.53	0.5034	4.32	103.53	0.0	0.0183
8-c	1.35	0.67	0.54	0.4963	4.32	111.76	0.0	0.0196
8-d	1.35	0.88	0.585	0.5037	4.32	117.65	0.0	0.0207
8-e	1.35	0.685	0.54	0.5074	4.32	110.58	0.0	0.0197
Average		0.68	0.55	0.6039	4.32	110.58	0.0	0.0196
Thickness (b) =0.65 inches								

TABLE IV. (continued)

DATA FOR SPECIMEN USED (GROUP II)

No. of Specimen	Height d	Final Cracks Length cf	Original Cracks Length c	Uncracked Height cf-c	Penetration Ratio c/d	Max. Load p	Distance Between Supports L	Displacement δ
V 1-a	o.277	0.255	0.125	0.140	0.4513	13.84	0.97	0.0248
V 1-b	0.278	0.257	0.127	0.130	0.4568	13.90	0.97	0.0149
V 1-c	0.275	0.262	0.127	0.135	0.4618	14.92	0.97	0.0148
V 1-d	o.285	0.269	0.129	0.140	0.4526	13.2	0.97	0.010
U 1-e	0.290	0.290	0.134	0.156	0.4621	20.0	1.05	0.0164
U 1-f	0.295	0.295	0.133	0.162	0.4508	20.0	1.05	0.0164
U 1-g	0.293	0.293	0.135	0.158	0.4608	21.5	1 05	o.0166
U 1-h	0.280	0.280	0.135	0.145	0.4821	17.0	1.05	0.0174
I 1-i	0.295	0.295	0.054	0.241	0.1831	34.25	1.05	0.0139
I 1-j	0.295	0.280	0.140	0.140	0.4746	16.9	1.05	0.0143
U 1-0	(Average)				0.4639	19.62		
V 1-0	"				0.4556	13.96		
I 1-0	"				0.3288	25.57		
Average	0.286		0.124	0.150	0.4161	18.55		0.0160

Thinckness (b) =0.148

TABLE IV (continued)(GROUP II)

V 2-d	0.424	0.412	0.220	0.192	0.5189	23.50	1.54	0.0160
U 2-e	0.422	0.420	0.225	0.195	0.5322	21.50	1.54	0.0133
U 2-g	0.422	0.412	0.210	0.182	0.4976	25.00	1.54	0.0200
I 2-i	0.423	0.410	0.257	0.153	0.6076	14.20	1.54	0.0175
I 2-j	0.423	0.410	0.221	0.189	0.5225	21.20	1.54	0.0139
U (Average)					0.5154	23.25		
V "					0.5189	23.50		
I "					0.5650	17,70		
Average	0.423		0.227	0.180	0.5330	21.08		0 0193
V 3-a	0.600	0.495	0.296	0.199	0.4933	28.90	2.10	0.0090
V 3-b	0.598	0. 468	0. 304	0.164	0. 5084	28.60	2.10	0.0080
V 3-c	0.595	0.466	0.303	0.163	0. 5092	30. 40	2.10	0.0118
V 3-d	0.595	0.473	0.305	0.168	0.5126	26.30	2.10	0.0088
U 3-e	0.602	0.583	0.288	0.295	0.4784	39.00	2.10	0.0209
U 3-f	0. 597	0.554	0.283	0.271	0.4740	40.50	2.10	0.0172
U 3-h	0.597	0.570	0.286	0.284	0.4791	40.50	2.10	0.0088
I 3-i	0.595	0.573	0.265	0.308	0.4454	46.50	2.10	0.0182
I 3-j	0.597	0.560	0.296	0.264	0.4958	42.10	2.10	0.0100
I 3-k	0.600	0.572	0.257	0.315	0.4283	44.40	2.10	0.0186
I 3-l	0.600	0.579	0.280	0.299	0.4667	42.00	2.10	0.0107
U (Average)					0.4726	39.75		
V "					0.5058	28.55		
I "					0.4630	43.10		
Total average			0.287	0.220	0.4800	37.20		

Thickness (b) = 0.303 inches

TABLE IV (continued)(GROUP II)

V 4-a	0.760	0.555	0.379	0.176	0.4987	41.50	2.56	0.0088
V 4-b	0.760	0.650	0.390	0.260	0.5131	53.50	2.56	0.0105
V 4-c	0.760	0.636	0.383	0.253	0.5039	53.00	2.56	0.0138
U 4-d	0.759	0.673	0.373	0.300	0.4914	61.00	2.56	0.0138
U 4-e	0.760	0.696	0.375	0.321	0.4934	55.00	2.56	0.0143
U 4-f	0.757	0.712	0.383	0.329	0.5060	57.20	2.56	0.0128
U 4-g	0.760	0.710	0.379	0.335	0.4987	57.00	2.56	0.0162
I 4-h	0.758	0.654	0.378	0.276	0.4987	54.20	2.56	0.0120
I 4-i	0.760	0.625	0.380	0.245	0.5000	57.80	2.56	0.0130
I 4-i	0.760	0.646	0.336	0.310	0.4421	64.20	2.56	0.0127
I 4-k	0.758	0.650	0.318	0.332	0.4195	68.20	2.56	0.0129
V 4-l	0.760	0.614	0.381	0.233	0.5013	46.50	2.56	0.0129
U (average)					0.4973	57.55		
V (average)					0.5032	48.63		
I "					0.4650	61.50		
Total average			0.371	0.280	0.4885	55.74		0.0128
Thickness (b) = 0.370 inches								
V 5-a	0.853	0.743	0.445	0.289	0.5217	52.20	2.99	0.0117
V 5-b	0.850	0.735	0.433	0.301	0.5106	59.10	2.99	0.0141
V 5-c	0.845	0.743	0.422	0.321	0.4994	61.20	2.99	0.0128
V 5-d	0.855	0.723	0.434	0.293	0.5076	58.10	2.99	0.0129
U 5-e	0.853	0.805	0.425	0.380	0.4982	71.60	2.99	0.0231
U 5-f	0.850	0.802	0.420	0.382	0.4941	69.00	2.99	0.0249
U 5-g	0.850	0.810	0.422	0.388	0.4965	68.00	2.99	0.0257
U 5-h	0.854	0.808	0.422	0.386	0.4941	68.10	2.99	0.0249

TABLE IV (continued) (GROUP II)

I 5-i	0.853	0.741	0.395	0.346	0.4631	74.10	2.99	0.0159
I 5-j	0.854	0.725	0.390	0.335	0.4572	68.90	2.99	0.0146
I 5-l	0.850	0.789	0.390	0.399	0.4588	73.20	2.99	0.0157
U (average)					0.4957	69.18		
V	"				0.5098	57.65		
I	"				0.4618	72.15		
Total average			0.416	0.350	0.4891	66.24		0.0177
Thickness (b) =0.430 inches								
V 6-a	1.067	0.941	0.521	0.420	0.4883	88.20	3.68	0.0118
V 6-b	1.067	0.935	0.545	0.390	0.5108	84.00	3.68	0.0156
V 6-c	1.061	0.875	0.533	0.342	0.5024	81.00	3.68	0.0101
V 6-d	1.070	0.920	0.520	0.400	0.4860	85.50	3.68	0.0116
U 6-e	1.063	1.063	0.515	0.548	0.4845	114.00	3.68	0.0241
U 6-f	1.060	1.060	0.510	0.550	0.4811	121.00	3.68	0.0290
U 6-g	1.070	1.070	0.526	0.544	0.4916	112.00	3.68	0.0285
U 6-h	1.070	1.017	0.514	0.503	0.4804	103.20	3.68	0.0229
I 6-i	1.069	0.961	0.514	0.447	0.4808	92.00	3.68	0.0169
I 6-j	1.065	0.875	0.504	0.371	0.4732	88.60	3.68	0.0141
I 6-k	1.069	0.955	0.530	0.425	0.4958	91.00	3.68	0.0170
U (average)					0.4844	112.55		
V	"				o.4968	84.67		
I	"				0.4792	91.65		
Total average			0.519	0.450	0.4868	96.50		0.0193
Thickness (b) =0.539 inches								

TABLE IV (continued) (GROUP II)

U 7-a	1.205	1.129	0.595	0.534	0.4938	121.0	4.24	0.0223
U 7-b	1.200	1.090	0.600	0.490	0.5000	124.0	4.24	0.0267
U 7-c	1.200	1.174	0.600	0.574	0.5000	122.20	4.24	0.0408
U 7-d	1.201	1.201	0.596	0.605	0.4963	128.20	4.24	0.0494
I 7-e	1.203	1.203	0.544	0.659	0.4522	192.00	4.24	0.0305
I 7-f	1.204	1.165	0.597	0.568	0.4958	120.00	4.24	0.0177
I 7-g	1.202	1.102	0.578	0.524	0.4809	136.00	4.24	0.0213
I 7-h	1.206	1.110	0.602	0.508	0.5033	121.0	4.24	0.0209
V 7-i	1.196	1.079	0.600	0.479	0.5017	109.0	4.151	0.0198
V 7-j	1.204	1.085	0.604	0.481	0.5017	115.6	4.151	0.0197
V 7-k	1.196	1.092	0.600	0.492	0.5017	115.6	4.151	0.0210
V 7-l	1.203	1.142	0.604	0.538	0.5020	121.20	4.151	0.0265
U (Average)					0.4975	123.85		
V "					0.5017	115.20		
I "					0.4830	142.25		
Total average			0.593	0.530	0.4940	127.10		0.0264
Thickness (b) =0.675 inches								
U 8-a	1.342	1.342	0.655	0.687	0.4880	158.0	4.70	0.0327
U 8-b	1.345	1.272	0.657	0.615	0 4885	143.2	4.70	0.0265
U 8-c	1.347	1.347	0.650	0.697	0.4826	153.0	4.70	0.0298
I 8-d	1.347	1.177	0.656	0.521	0.4870	126.2	4.70	0.0218
I 8-e	1.350	1.205	0.708	0.497	0.5244	122.4	4.70	0.0147
I 8-f	1.342	1.170	0.688	0.482	0.5127	117.0	4 70	0.0163
I 8-g	1.347	1.159	0.630	0.529	0.4677	139.0	4.70	0 0214
V 8-h	1.295	1.094	0 600	0.494	0.4633	125.0	4 70	0.0202

TABLE IV. (GROUP II continued)

V 8-i	1.290	1.010	0.606	0.404	0.4698	120.0	4.70	0.0154
V 8-j	1.291	1.023	0.595	0.428	0.4609	115.0	4.70	0.0141
V 8-k	1.290	1.055	0.605	0.450	0.4689	116.0	4.70	0.0132
U 8-1	1.347	1.347	0.667	0.680	0.4951	168.0	4.70	0.0341
U (Average)					0.4885	155.5	4.70	
V "					0.4657	119.0		
I "					0.4979	126.15		
Total average			0.463	0.540	0.4840	133.55		0.0217

Thickness (b) =0.675 inches

TABLE IV. (continued)

DATA FOR SPECIMEN USED
(GROUP III)

No. of Specimen	Height	Original Crack	Uncracked Height	Penetration Ratio	Distance Between Supports	Max. Load	Residual Load	Displacement
	d (inch)	C (inch)	d-C (inch)	C/d	L (inch)	P (lb)	P (lb)	δ (inch)
U a-1	0.406	0.100	0.306	0.2463	2.60	6.9	0.0	0.0253
U a-2	0.393	0 100	0.293	0.2544	2.60	12.8	0.0	0.0311
U a-3	0.406	0.100	0.306	0.2463	2.60	12.5	0.0	0.0290
U a-4	0.407	0.100	0.307	0.2457	2.60	11.6	0.0	0.0288
U a-5	0.412	0.100	0.312	0.2427	2.60	11.2	0.0	0.0248
U a-6	0.408	0.100	0.308	0.2450	2.60	12.4	0.0	0.0276
V a-7	0.411	0.100	0.311	0.2433	2.60	11.1	0.0	0.0221
V a-8	0.412	0.100	0.312	0.2427	2.60	11.2	0.0	0.0230
V a-9	0.420	0.100	0.320	0.2380	2.60	10.2	0.0	0.0219
V a-10	0.414	0.100	0.314	0.2415	2.60	10.3	0.0	0.0207
V a-11	0.406	0.100	0.306	0.2463	2.60	10.7	0.0	0.0219
V a-12	0.408	0.100	0.308	0.2450	2.60	9.8	0.0	0.0223

TABLE IV. (continued) (GROUP III)

I a-13	o.414	0.100	0.318	0.2415	2.60	9.7	0.0	0.0207
I a-14	0.405	0.100	0.305	0.2469	2.60	8.94	0.0	0.0184
I a-15	0.407	0.100	0.307	0.2457	2.60	10.74	0.0	0.0225
I a-16	0.406	0.104	0.302	0.2463	2.60	12.0	0.0	0.0324
I a-17	0.411	0.100	0.311	o.2433	2.60	11.8	0.0	0.0230
I a-18	0.392	0.107	0.285	0.2551	2.60	10.63	0.0	0.0237
U (average)		0.100	0.357	0.2467	2.60	11.23		
V "		0.100	0.312	0.2428	2.60	10.545		
I "		O.102	0.305	0.2465	2.60	10.60		
Total average		0.1006	0.307	0.2453	2.60	10.925		0.0244
Thickness (b) =0.1 Inches								
U b-1	0.407	0.134	0.273	0.3292	2.60	10.0	0.0	o.0212
U b-2	0.414	0.134	0.280	0.3236	2.60	10.0	0.0	0.0182
U b-3	0.407	0.134	0.273	0.3292	2.60	9.6	0.0	0.0198
U b-4	0.416	0.134	0.234	0.3221	2.60	9.6	0.0	0.0173
U b-5	0.405	0.134	0.271	0.3308	2.60	9.3	0.0	0.0186
U b-6	0.412	0.134	0.305	0.3252	2.60	9.74	0.0	0.0182
V b-7	0.409	0.134	0.275	0.3276	2.60	9.81	0.0	0.0186
V b-8	0.418	0.134	0.248	0.3205	2.60	11.3	0.0	0.0200
V b-9	0.416	0.134	0.234	0.3221	2.60	9.68	0.0	0.0175
V b-10	0.414	0.134	0.280	0.3198	2.60	9.71	0.0	0.0173
V b-11	0.419	0.134	0.285	0.3198	2.60	11.01	0.0	0.0184
V b-12	0.403	0.134	0.269	0.3225	2.60	9.61	0.0	0.0207
I b-13	0.405	0.137	0.268	0.3382	2.60	8.39	0.0	0.0184
I b-14	0.416	0.125	0.290	0.3012	2.60	11.0	0.0	0.0175
I b-15	0.411	0.125	0.286	0.3041	2.60	10.28	0.0	0.0166

TABLE IV. (continued) (GROUP III)

I b-16	0.411	0.125	0.286	0.3041	2.60	9.34	0.1	0.0152
I b-17	0.410	0.141	0.269	0.3439	2.60	8.62	0.0	0.0162
I b-18	0.402	0.279	0.279	0.3059	2.60	9.60	0.0	0.0156
U (average)		0.134	0.273	0.3267		9.71		
V "		0.134	0.265	0.3221		1o.19		
I "		0.129	0.280	0.3217		9.811		
Total average		0.132	0.273	0.3217		9.811		0.0181
Thickness (b) =0.1 inches								
U c-1	0.409	0.200	0.209	0.4889	2.60	6.0	0.00	0.0175
U c-2	0.406	0.200	0.206	0.4926	2.60	5.6	0.05	0.0173
U c-3	0.411	0.200	0.211	0.4866	2.60	5.03	0.25	0.0133
U c-4	0.418	0.200	0.218	0.4784	2.60	6.45	0.0	0.0168
U c-5	0.407	0.200	0.207	0.4914	2.60	5.3	0.31	0.0156
U c-6	0.406	0.200	0.206	0.4926	2.60	5.86	0.20	0.0179
V c-7	0.420	0.200	0.220	0.4761	2.60	6.46	0.40	0.0150
V c-8	0.390	0.200	0.190	0.5128	2.60	4.65	0.05	0.0161
V c-9	0.393	0.200	0.193	0.5089	2.60	5.41	0.05	0.0173
V c-10	0.419	0.200	0.219	0.4773	2.60	5.75	0.05	0.0161
V c-11	0.409	0.200	0.209	0.4889	2.60	5.79	0.08	0.0152
V c-12	0.410	0.200	0.210	0.4878	2.60	5.75	0.24	0.0141
I c-13	0.399	0.200	0.199	0.5012	2.60	5.17	0.05	0.0138
I c-14	0.414	0.175	0.239	0.4227	2.60	7.40	0.25	0.0150
I c-15	0.410	0.200	0.210	0.4887	2.60	7.25	0.0	0.0200
I c-16	0.416	0.220	0.196	0.5288	2.60	5.32	0.05	0.0138

TABLE IV. (continued) (GROUP III)

I c-17	0.415	0.200	0.215	0.4819	2.60	6.85	0.0	0.0161
I c-18	0.410	0.192	0.218	0.4682	2.60	6.08	0.20	0.0172
U (average)		0.200	0.210	0.4884		5.706		
V "		0.200	0.207	0.4919		5.636		
I "		0.198	0.213	0.4818		6.345		
Total average		0.199	0.209	0.4874		5.896		0.0158
Thickness (b) =0.1 inches								
d-1	o.460	0.05	0.410	0.1087	3.60	14.22	0.0	0.0638
d-2	0.460	0.05	0.410	0.1o87	3.60	14.52	0.0	0.0667
d-3	0.461	0.05	0.411	0.1o84	3.60	14.21	0.0	0.0682
d-4	0.450	0.05	0.400	0.1111	3.60	14.71	0.0	0.0725
d-5	0.460	0.05	0.410	0.1087	3.60	13.38	0.0	0.0580
d-6	0.440	0.05	0.390	0.1136	3.60	12.90	0.0	0.0580
d-7	0.460	0.05	0.410 .	0.1087	3.60	15.52	0.0	0.0667
Average	0.456	0.05	0.405	0.1097	3.60	14.35		0.0648
Thickness (b) =0.1 inches								
e-1	0.490	0.10	0.390	0.2040	3.60	11.08	0.0	0.0479
e-2	0.491	0.10	0.391	0.2036	3.60	10.74	0.0	0.0450
e-3	0.492	0.10	0.392	0.2032	3.60	11.82	0.0	0.0696
e-4	0.494	0.10	0.394	0.2024	3.60	11.64	0.0	0.0479
e-5	0.486	0.10	0.386	0.2058	3.60	11.73	0.0	0.0479
e-6	0.491	0.10	0.391	0.2037	3.60	13.00	0.0	0.0537
e-7	0.488	0.10	0.388	0.2049	3.60	12.60	0.0	0.0493

TABLE IV. (continued) (GROUP III)

Average								
	0.490	0.10	0.390	0.2039	3.60	11.80		0.0585
Thickness (b) =0.10 inches								
f-1	0.608	0.20	0.408	0.3289	3.60	10.40	0.3	0.0276
f-2	0.610	0.20	0.410	0.3279	3.60	10.10	0.8	0.0261
f-3	0.613	0.20	0.413	0.3262	3.60	13.60	0.0	0.0348
f-4	0.610	0.20	0.410	0.3279	3.60	10.93	0.45	0.0290
f-5	0.609	0.20	0.409	0.3284	3.60	10.50	0.60	0.0305
f-6	0.610	0.20	0.410	0.3279	3.60	9.40	1.18	0.0261
f-7	0.612	0.20	0.412	0.3268	3.60	12.60	0.0	0.0319
Average								
	0.610	0.20	0.410	0.3277	3.60	11.075		0.0294
Thickness (b) = 0.10 inches								
g-1	0.704	0.287	0.417	0.4077	3.60	10.58	1.8	0.0241
g-2	0.700	0.300	0.400	0.4286	3.60	11.95	0.25	0.0296
g-3	0.707	0.300	0.407	0.4243	3.60	9.64	1.29	0.0218
g-4	0.701	0.300	0.401	0.4280	3.60	9.00	1.18	0.0232
g-5	0.708	0.300	0.408	0.4237	3.60	9.82	0.65	0.0247
g-6	0.706	0.292	0.414	0.4136	3.60	10.50	0.35	0.0247
g-7	0.709	0.297	0.412	0.4189	3.60	11.69	0.20	0.0281
Average								
	0.705	0.297	0.408	0.4210		10.453		0.0252
Thickness (b) = 0.10 inches								

TABLE IV. (continued) (GROUP III)

h-1	0.825	0.400	0.425	0.4848	3.60	11.90	0.35	0.0261
h-2	0.820	0.400	0.420	0.4878	3.60	11.82	0.35	0.0255
h-3	0.816	0.403	0.413	0.4939	3.60	13.58	0.20	0.0276
h-4	0.817	0.414	0.403	0.5067	3.60	11.66	0.15	0.0247
h-5	0.820	0.412	0.408	0.5024	3.60	11.85	0.22	0.0261
h-6	0.814	0.401	0.412	0.4926	3.60	12.40	0.22	0.0261
h-7	0.816	0.400	0.416	0.4902	3.60	11.43	0.18	0.0278
Average:								
	0.818	0.404	0.414	0.4940		12.05		0.0263
Thickness (b) =0.10 inches								
i-1	0.915	0.500	0.415	0.5464	3.60	12.20	0.25	0.000
i-2	0.904	0.500	0.404	0.5531	3.60	10.60	0.50	0.0218
i-3	0.911	0.495	0.416	0.5434	3.60	11.00	0.25	0.0232
i-4	0.913	0.501	0.412	0.5487	3.60	11.96	0.0	0.0238
i-5	0.914	0.500	0.414	0.5470	3.60	12.00	0.0	0.0232
i-6	0.924	0.500	0.424	0.5411	3.60	12.08	0.22	0.0261
i-7	0.925	0.506	0.419	0.5470	3.60	12.70	0.12	0.0261
Average:								
	0.915	0.500	0.414	0.5470		11.79		0.0238
Thickness (b) =0.10 inches								
j-1	0.977	0.611	0.366	0.6254	3.60	7.82	0.50	0.0174
j-2	0.966	0.600	0.366	0.6211	3.60	9.40	0.00	0.0189
j-3	0.961	0.610	0.351	0.6348	3.60	8.15	0.25	0.0189
j-4	1.000	0.601	0.399	0.6010	3.60	11.50	0.35	0.0209

TABLE IV. (continued) (GROUP III)

j-5	0.973	0.579	0.394	0.5951	3.60	8.25	1.50	0.0174
j-6	0.998	0.602	0.396	0.6032	3.60	12.00	0.12	0.0218
j-7	1.070	0.606	0.464	0.5663	3.60	12.10	0.10	0.0247
j-8	0.923	0.600	0.323	0.6500	3.60	8.50	0.12	0.0250
Average								
	0.987	0.601	0.382	0.6120		9.715		0.0206

Thickness (b) = 0.10 inches

TABLE V.

RESULTS OF SURFACE ENERGY CALCULATION BY USING DIFFERENT EQUATIONS (GROUP I)

	Equations for Surface energy calculation $(erg/cm^2).(10)^5$							
Specimen	1	11	111	1V	V	V1	V11	V111
1	2.15	2.074	28.80	5.74	6.89	1.656	o. 018	1. 86
2	2.16	2.160	29.90	6.172	9.69	2. 822	0. 055	2. 024
4	2.40	2.40	31. 93	6.64	9.32	2. 84	0.147	2. 094
5	2. 425	2.425	40. 89	7. 46	8. 886	3. 051	0. 205	2. 023
6	2.17	2.17	42. 87	7. 898	9. 59	3. 552	0. 297	1. 738
7	2.11	2.11	68. 29	10. 00	7. 322	2. 094	0. 274	1. 358
8	2. 65	2. 65	56. 26	10. 52	11. 416	3. 164	0. 547	2. 092

TABLE V. (continued)

RESULTS OF SURFACE ENERGY CALCULATION BY USING DIFFERENT EQUATIONS

(GROUP II)

Specimen	Equations for Surface Energy Calculation (erg/cm^2). (10)^5							
	1	11	111	1V	V	V1	V11	V111
1 - U	6.160	6.160	52.77	13.903	28.98	7.048	0.077	7.689
- V	4.365	4.365	28.00	7.592	15.947	3.963	0.0432	7.958
- I	5.370	5.370	26.095	9.76	20.165	6.540	0.0535	5.466
Total	5.298	5.298	35.622	10.418	21.697	5.850	0.0597	7.038
2 - U	3.785	3.786	45.31	9.765	19.19	5.415	0.0995	2.750
- V	3.76	3.76	47.43	10.08	19.74	5,49	0.101	2.440
- I	2.920	2.920	43.24	7.64	13.66	3.445	0.064	2.378
Total	3.458	3.458	45.33	9.162	17.53	4.783	0.088	2.523
3 - U	3.475	3.475	30.76	7.745	15.95	3.96	0.177	5.298
- V	1.320	1.320	21.637	5.123	9.637	2.20	0.104	1.304
- I	2.582	2.582	32.618	8.546	17.72	4.556	0.195	2.798
Total	2.459	2.459	28.338	7.138	14.436	3.572	0.159	3.134

TABLE V. (GROUP II, continued)

4 - U	2.545	2.545	39.08	9.043	18.215	4.883	0.255	2.835
- V	1.770	1.770	30.34	6.803	13.567	3.560	0.207	1.887
- I	2.250	2.250	37.69	8.370	17.330	5.105	0.2877	2.213
Total	2.188	2.188	35.706	8.072	16.370	4.516	0.249	2.308
5 - U	4.045	4.045	39.66	9.273	18.65	5.590	0.381	5.549
- V	1.807	1.807	31.75	7.01	12.82	4.017	0.285	1.518
- I	2.522	2.522	30.95	7.495	17.160	5.657	0.383	2.281
Total	2.792	2.792	34.121	7.91	16.210	5.088	0.349	3.116
6 - U	4.378	4.378	46.14	11.30	23.080	6.207	0.259	5.372
- V	1.537	1.537	29.42	6.845	13.790	3 545	0.454	1.056
- I	2.627	2.627	28.95	7.210	14.810	3.997	0 508	3.272
Total	2 859	2 859	34 84	8 450	17 230	4 580	0.4.7	3.230
7 - U	5.203	5.203	49.23	11.39	22.94	6.033	0.927	7.970
- V	3.112	3.112	54.58	10.17	20.35	5.290	0.778	2.895
- I	4.048	4.048	44.64	12.88	28.22	7.87	1.224	3.199
Total	4.121	4.121	49.48	11.48	23.83	6.397	0.976	4.688
8 - U	4.470	4.470	51.32	12.06	23.28	6.113	1.246	5.833
- I	2.242	2.242	34.32	7.907	15.85	5 86	0.834	2.191
- V	1.737	1.737	25.18	6.580	13.71	5.63	0 774	1.573
Total	2.816	2.816	36.94	8.85	17.63	5.86	0.951	3.199

TABLE V. (continued)

RESULTS OF SURFACE ENERGY CALCULATION BY USING DIFFERENT EQUATIONS
(GROUP III)

	Equations for surface energy calculation(erg/cm^2)·(10^5)							
Specimen	I	II	III	IV	V	VI	VII	VIII
A - U	4.445	4.505	14.10	7.767	19.930	4.760	0.0260	15.050
- V	3.243	5.967	11.017	6.887	14.55	3.800	0.0213	9.384
- I	3.620	3.610	12.802	7.593	15.79	4.190	0.0228	11.040
Total	3.769	4.694	12.640	7.416	16.757	4.250	0.0234	11.824
B - U	2.942	2.942	23.080	9.657	19.473	5.012	0.029	6.380
- V	3.158	3.158	21.170	9.078	20.490	5.367	0.0313	6.229
- I	2.463	2.463	17.820	8.250	15.503	3.870	0.0262	4.940
Total	2.854	2.854	20.690	8.996	18.490	4.749	0.0288	5.873
C - U	1.958	1.902	31.600	7.593	15.456	4.270	0.0175	2.213
- V	1.848	1.805	32.430	7.661	15.461	4.248	0.0178	1.992
- I	1.998	1.980	36.510	8.918	18.201	5.155	0.0215	1.938
Total	1.953	1.896	33.510	8.057	16.357	4.557	0.0189	2.048

TABLE V. (GROUP III, continued)

D	10.018	10.018	6.804	7.600	16.504	4.378	0.0084	81.648
E	6.821	6.821	10.784	7.888	16.985	4.448	0.0183	23.947
F	3.498	3.361	15.671	6.944	15.010	3.297	0.0223	7.183
G	2.833	2.682	21.045	6.522	13.990	2.448	0.0182	3 896
H	3.350	3.282	36.200	8.484	16.610	2.456	0.0192	3.415
I	2.961	2.921	42.054	7.993	14.902	4.407	0.0148	2.504
J	2.295	2.261	48.95	7.023	10.916	2.706	0.0094	1.482

TABLE VI.

Surface energy of plexiglas

From Data by Rose and English (17)

Diameter of hole, in	Surface energy $erg/cm^2 \cdot 10^5$
1/4	7.8, 4.5, 7.3, 12.6, 2.8, 4.5, 11.3, 8.3, 4.5 8.9, 7.3, 4.9, 5.4, 6.3, 6.7
1/2	11.5, 5.2, 13.5, 6.8, 8.6, 9.4, 11.1, 4.9, 8.6
5/8	15.7, 5.2, 16.2, 7.6, 9.0, 14.9, 6.4, 10.2
3/4	15.4, 13.2, 9.1, 12.7, 9.1, 14.0, 14.0, 12.2
7/8	12.6, 14.7, 12.6, 14.7, 8.8, 19.5, 17.0, 14.0
1/1	23.2, 21.0, 15.0, 24.7, 31.2, 13.2, 20.9
3/2	55.9, 28.6, 22.9, 20.4, 20.3,36.5, 29.7

(II) Appendix II.

This appendix describes the factors affecting use of the crystal slicing instrument for cutting the wire saw notch into the specimen.

The wire saw notch was cut into the specimen using a Model SD-12A crystal slicing and dicing instrument. Reference is made to Figures for a photograph of the system, which is described below.

The specimen was held in the jaws of a clamp in a position perpendicular to the path of a thin wire blade.

The blade passed over a drive roller and three guide rollers to give a continuous cutting contact on the specimen surface.

Cutting was accomplished by an abrasive fed at the point of contact between the moving wire and the material being cut, the abrasive being imbedded in the soft wire and then cutting by chipping its way through the material.

Five factors were found to be important to the cutting life and cutting speed of the blades. They were the blade material, the slurry, the speed, the tension in the saw blade and the cutting pressure.

1. The blade material

Two types of blades were used

1. 0.01 " diameter nichrome
2. 0.01 " diameter stainless steel blades

The former worked well for this type of material (plexiglas), but the latter all broke in a relatively short time and no cuts were

completed.

2. The slurry

The slurry mixture used in this experiment was a mixture of 100 ml glycerine, 12 gm silicon carbide and 12 gm boron carbide together with 50 ml water. The abrasive slurry was fed by hand, from a plastic dropper bottle, onto the specimen at the point of blade contact. Larger grit did not give increased cutting speeds and had the effect of moving the blade out of the groove, especially under low cutting load.

In earlier experimentation the mixture may have been a cause of blade failure so to ensure thorough mixing the slurry was mechanically vibrated for about ten minutes before each use and this ceased to be a problem.

3. Speed

General speaking, the higher the speed, the straighter and more quickly the notch was made, but the wire strength decreased causing the wire to fail more easily. The speed initially tried was 25-35 of full speed, which gave a long blade life but yielded a low cutting rate. The wire speed was then changed and it was found that a 50% speed gave the optimum results for this type of material.

4. Tension in the saw blade

It was found necessary to maintain the blade tension at a

constant level, not too tight or too slack, as too high a tension in cutting can frequently lead to failure, a deflection of 3/8" when the blade touched the specimen was found satisfactory.

5. Cutting pressure

As the blade cuts into a material the load due to the weight increases as the arm comes down. To maintain a constant load it was therefore necessary to change the position of the weight on top of the arm. At the same time the load could not be reduced too far or the blade would not make a straight cut, but deflect away from the cutting plane.

Figure 34. Equipment for cutting wire saw notch into the specimen

(III) Appendix III.

This appendix contains the symbols used in this report

Symbols

	Surface energy
de	The release of strain energy
C	Original crack length
C_f	Final crack length
σ	Stress in the specimen
U	Elastic energy stored in the specimen
A	Area of the new fracture surface
δ	Deflection of the center of the specimen over the loading process
P	Load applied to the specimen
P_m	Load at failure
P_r	Residual load after crack growth
b	Thickness of specimen
L	Length between supports
d	Height of specimen
d-C	Uncracked height
C/d	Crack penetration ratio
M	Bending moment in the specimen
Y	Distance from the neutral axis to the required point

I	Moment of inertia of specimen around neutral axis
K_{ic}	Stress-intensity factor
G_{ic}	Strain-energy release rate
E	Youngs modulus of Specimen material
γ	Poissons' ratio of specimen material
K	Stiffness of the specimen

VI. BIBLIOGRAPHY

1. Griffith A. A., "The Phenomenon of Rupture and Flow in Solids", Phil. Trans. Roy. Soc. Lond. (1921) A 221, 163-198

2. Inglis C. E., "Stresses in a Plate due to the presence of Crack and Sharp Corners", Trans. Inst. Naval Architects, (1913) 60, 219-239.

3. Brace W. F., & Walsh S. B., "Some Direct Measure ments of the Surface Energy of Quartz and Orthoclase", Amer. Min. 47, (1962) 1111-1122.

4. Gilman J. J., "Direct Measurements of the Surface Energy of Crystal", J. Appl. Phys. 31 (1960), 2208-2218

5. Chang Lo-Ching, J. Mech. Phys. Solids, 3 (1955), 212.

6. Gilman, J. J., Knudsen C. and Walsh W. P., J. Appl. Phys. 29 (1958), 601

7. Irwin, G. R., Report No. 5486. U. S. Naval Research Laboratory, Washington, D. C. (1960a).

8. Sullivan, R. M., "New Specimen design for Plane-Strain Fracture Toughness Tests" Maths. Res. & Standards (1964) 4 (1), 20-24.

9. Brown, W. F., Jr., & Srawley, J. E.,"Plane strain crack Toughness testing", SP 410. ASTM, Philadelphia(1966)

10. Summers, D. A., Personal communication.

11. Liebowitz, H., Vanderveldt, H., & Harris, D. W. Intern. J. Solids and Structures. (1967b), 3, 489

12. Paris, P. C., & Sih, G., "Symposium of Fracture Toughness Testing and Its Applications", STP 381 30-81, Philadephia (1965)

13. Bueckner, H. F. , "Some Stress Singularities and Their Computation by means of Integral Equations!' "Boundary value Problems in Differential Eq." Univ. of Wisconsin Press, Madison, (1960).

14. Srawley, J. E., & Brown, W. F., Jr"Symposium on Fracture Toughness Testing and Its Applications", STP 381 133-195, ASTM, Philadelphia (1965)

15. Gross, B. & Srawley, J. E., (1967). Mater. Res. Std. 7.155.

16. Davidge, R. W. & Tappin, G., "The Effective Surface Energy of Brittle Materials", J. Mater. Sci. 3, (1968) 165.

17. Rose, H. E., & English, J. E. , "Bending of Slotted Beams as a means of determination of Surface Energy", Trans. Instn. Min. Metall. (Sect. C. Mineral Process. Extr. Metall.). Dec. 1968, 191-194

18. Bieniawski Z. T., "Mechanism of Brittle Fracture of Rock, "

Int. J. Rock Mech. Min. Sci. Vol. 4, 395-406.

19. Schardin, H. "Velocity Effects in Fracture" in Fracture ed. Averbach. (1959) paper 12.

20. Wiederhorn, S. M., "Influence of Water Vapor on Crack Propagation in Soda lime glass". Am. Cer. Soc. J. (1967) Aug. 50 (8) 407-414.

VII. VITA

The author, Li-King Chen, was born on December 7, 1938 in Szuchuan, China. He received his elementary and high school education in Kaohsiung, Taiwan. In June, 1966 he graduated from Taiwan Provincial Cheng Kung University with a degree of Bachelor of Science in Mining Engineering. From June, 1965 to March, 1966 he was employed by the "Keng Da Coal Mining Company" in Keelung, Taiwan.

He entered the University of Missouri at Rolla in September, 1968 as a graduate student in the Department of Mining Engineering.